

Alma Mater Studiorum – Università di Bologna

DOTTORATO DI RICERCA IN

Scienze Farmacologiche e Tossicologiche, dello
sviluppo e del movimento umano

Ciclo XXIX

Settore Concorsuale di afferenza: 05/G1

Settore Scientifico disciplinare: BIO/14

NEUROPROTECTIVE STRATEGIES IN NEURODEGENERATIVE DISORDERS

Presentata da: Dott. Massimo D'Amico

Coordinatore Dottorato

Prof.ssa Patrizia Hrelia

Relatore

Prof. Andrea Tarozzi

Esame finale anno 2017

TABLE OF CONTENTS

Part 1. TARGETING NRF2 PATHWAY FOR NEUROPROTECTION AND REDUCTION LEVODOPA-INDUCED TOXICITY IN PARKINSON'S DISEASE.

Chapter 1. <u>INTRODUCTION</u>	5
1.1 PARKINSON'S DISEASE	5
1.2 EPIDEMIOLOGY AND INCIDENCE	6
1.3 ORIGIN AND RISK FACTORS	7
1.4 SYMPTOMATOLOGY	9
1.5 THERAPEUTIC STRATEGIES	10
Chapter 2. <u>METHODS</u>	14
2.1 CELL CULTURE	14
2.2 L-DOPA	14
2.3 SULFORAPHANE	14
2.4 DETERMINATION OF CELL PROLIFERATION	14
2.5 APOPTOSIS ASSAY	15
2.6 DETERMINATION OF INTRACELLULAR GLUTATHIONE LEVELS	16
2.7 ELISA ASSAY FOR ACTIVATED NRF2 TRANSCRIPTION FACTOR	17
2.8 QUANTITATIVE REAL-TIME PCR	18
Chapter 3. <u>RESULTS</u>	19
3.1 NEUROTOXIC EFFECTS OF L-DOPA	19
3.2 SULFORAPHANE COUNTERACT THE NEUROTOXOCITY INDUCED BY L-DOPA	19
3.3 SULFORAPHANE PREVENTS THE NEUROTOXOCITY INDUCED BY L-DOPA	21
3.4 THE COMBINATION OF SFN AND L-DOPA PREVENTS THE APOPTOSIS INDUCED BY H₂O₂	22
3.5 SFN POTENTIATES THE INCREASE OF NRF2 mRNA AND NRF2-ARE BINDING ACTIVITY INDUCED BY L-DOPA.	23
3.6 SFN POTENTIATES THE INCREASE OF GSH INDUCED BY L-DOPA	24
Chapter 4. <u>DISCUSSION</u>	26

Part 2. KNOCK-OUT OF A MITOCHONDRIAL SIRTUIN PROTECTS NEURONS FROM DEGENERATION IN *C. elegans*

Chapter 1. <u>INTRODUCTION</u>	30
1.1 STROKE	30
1.2 MOLECULAR MECHANISMS OF CELL DEATH IN STROKE	31
1.3 DEG/ENaC CHANNELS TOXICITY	33
1.4 CHEMICAL ISCHEMIA	35
1.5 SIRTUINS	36

1.5.1 MAMMALIAN SIRTUINS	36
1.5.2 THE NUCLEAR SIRTUINS SIRT1, SIRT6, SIRT7	38
1.5.3 THE CYTOPLASMIC SIRTUIN SIRT2	39
1.5.4 THE MITOCHONDRIAL SIRTUINS SIRT3, SIRT4, SIRT5	40
1.5.5 <i>Caenorhabditis elegans</i> SIRTUINS	43
1.6 CALORIC RESTRICTION	44
1.7 SIRTUIN IN CALORIC RESTRICTION	45
1.8 OXIDATIVE STRESS AND MITOHORMESIS	46
1.9 THE MODEL ORGANISM <i>Caenorhabditis elegans</i>	47
Chapter 2. <u>METHODS</u>	49
2.1 CAENORHABDITIS ELEGANS STRAINS AND GROWTH	49
2.2 MOLECULAR BIOLOGY	50
2.3 NEMATODE SYNCHRONIZATION	50
2.4 FLUORESCENT MICROSCOPY	50
2.5 CHEMICALLY INDUCED ISCHEMIA AND QUANTIFICATION OF NEURONAL DEATH	51
2.6 CAENORHABDITIS <i>ELEGANS</i> EMBRYONIC CELL CULTURE	51
2.7 QUANTITATIVE REAL-TIME PCR	53
2.8 QUANTIFICATION OF ROS	53
2.9 SAMPLE SIZE AND DATA REPLICATION	54
2.10 STATISTICS	55
Chapter 3. <u>RESULTS</u>	56
3.1 LONG LASTING PROTECTION OF DIAPAUSE AGAINST <i>mec-4(d)</i> AND <i>mec-10(d)</i> INDUCED NEURONAL DEATH	56
3.2 KNOCK-OUT OF A MITOCHONDRIAL SIRTUIN IS PROTECTIVE AGAINST NEURONAL DEATH	58
3.3 KNOCK-OUT OF <i>sir-2.3</i> IS PROTECTIVE IN HYPERACTIVE MEC CHANNEL INDUCED NEURONAL DEATH	63
3.4 BLOCK OF THE NICOTINAMIDE ADENINE DINUCLEOTIDE (NAD) SALVAGE PATHWAY PROTECTS AGAINST NEURONAL DEATH	66
3.5 BLOCK OF GLUCOSE METABOLISM REDUCES <i>mec-4(d)</i> INDUCED NEURONAL DEATH	67
3.6 EXPERIMENTS IN CELL CULTURE REVEAL A CELL AUTONOMOUS EFFECT OF 2-DG DEPENDENT ON KNOCK-OUT OF <i>sir-2.3</i>	69
3.7 MITOHORMETIC ELEVATION OF ROS AND PROTECTION AGAINST NEURONAL DEGENERATION	72
Chapter 4. <u>DISCUSSION</u>	75
4.1 INSIGHTS INTO THE ROLE OF MITOHORMETIC ROS IN NEURONAL PROTECTION MEDIATED BY HYPERACTIVE CHANNELS IN ISCHEMIA	75
4.2 KNOCK-OUT OF MITOCHONDRIAL SIRTUIN <i>sir-2.3</i> AND ROS	76
Chapter 5. <u>BIBLIOGRAPHY</u>	80

PART I

**TARGETING NFR2 PATHWAY FOR NEUROPROTECTION AND
REDUCTION LEVODOPA-INDUCED TOXICITY IN PARKINSON'S
DISEASE.**

1. INTRODUCTION

1.1 PARKINSON'S DISEASE

Parkinson's disease (PD) is a neurodegenerative disorder characterized by a progressive loss of dopaminergic neurons in the substantia nigra pars compacta (SNpc). The most dramatic loss of dopaminergic neurons within the SNpc is typically in the ventrolateral tier, which is probably the cause of the motor impairment. The resultant lacking of dopamine leads to a "parkinsonism," a characteristic symptomatology that includes bradykinesia, muscular rigidity, rest tremor and postural impairment[1].

Lewy bodies are also the hallmark unique of this pathology, composed by insoluble and aggregated oligomers of α -synuclein within the cell body and the processes of neurons. This feature could also be found not only in the brain but including the spinal cord and peripheral nervous system[2].

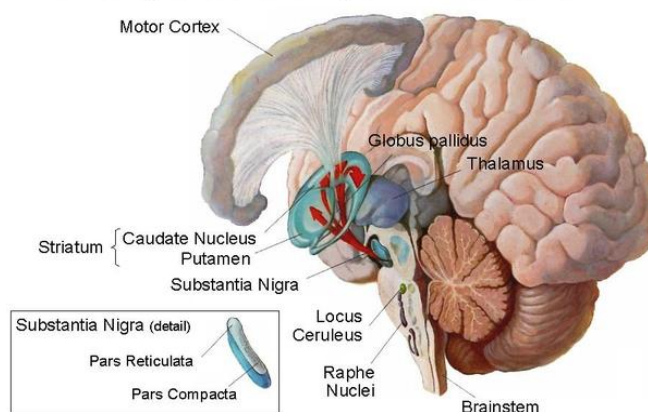


Figure.1 Brain regions affected by Parkinson's Disease

Many processes are implicated in the onset of the pathology like oxidative stress, mitochondrial impairments, inflammation, excitotoxicity and protein aggregates. The principal component of LBs inclusions is α -synuclein, which operates a major role in the pathogenesis of this disease. The physiological function of α -synuclein and the mechanism that mutations in this gene lead to neurons loss are still not clear, although it has been observed that an excess of α -syn depositions can cause dopaminergic neurons loss[3]. On the other hand, oxidative damage induced by reactive oxygen species (ROS) participates in the progression of dopaminergic neurons degeneration. In particular, the metabolism of dopamine (DA) might be able to raise basal levels of oxidative stress; indeed, dopamine oxidation leads to the formation of neurotoxic species[4].

1.2 EPIDEMIOLOGY AND INCIDENCE

PD is a progressive disease with a mean age at onset of 55, the pathology's prevalence increases to 1% in persons 65 years old, this percentage reach 3% in individuals with age over 85 without a notable difference by the sex. In about 95% of cases, PD is idiopathic multifactorial disease due to environmental agents and genetic susceptibility; there is no apparent familiar genetic bond; these cases are indicated as "sporadic" PD[5]. On the other hand, residual 5% cases are the consequence of genetic mutations and are inherited. Normally, the pathology is diagnosed about 60 years of age, but in 10% of cases the onset would be earlier around 45 years, this is recognized by the scientific community like precocious incidence.

The prevalence and the incidence of PD increase with age, the increase of the life expectancy coupled with the demographic shift in the population could explain the

rising number of cases seen worldwide. However, in the last two decades, it was observed a gradual raise in the mean age at onset of the disease and this feature is not entirely explained by population aging, but suggest that presumably additional variables may play a central role[6]. Reasonably, the increasing knowledge of the neurodegenerative chronic diseases, the development of the accuracy of diagnosis could be linked to these cases. In fact, early physical traits that in the past were related to aging or missed by older patients now are more related to the medical corps. This circumstance could also be defined by a reduction of cases of precocious incidence.

1.3 ORIGIN AND RISK FACTORS

Parkinson's disease is a pathology that in the 85% of the cases has a sporadic origin. Moreover, in about 15% of the cases, is linked to genetic causes[7]. The genes involved are called PARKs, which include six members. The transmission of these genes it is either autosomal dominant for α -synuclein, UCHL1, and LRRK2 or autosomal recessive transmission for parkin, DJ-1, and PINK-1. The recessive form is characterized by an early onset, and it usually shows the most severe outcome. Among the six proteins engaged in the familial forms of PD, α -syn is clearly the most studied, not only because was the first gene identified, but also because is the major fibrillar protein of the Lewy bodies[8].

There are several dysfunctions noticed in PD, excitotoxicity, mitochondrial impairments and oxidative stress, that lead to cellular death. Oxidative stress is due to a disequilibrium between the levels of ROS produced and eliminated. ROS are produced by many pathways such as the activation of enzymes like adenine dinucleotide phosphate oxidase (NADPH) and nitric oxide synthase (NOS). The

massive production of ROS in the brain may give an explanation for the degree of the role that these reactive molecules operate in PD[9]. The brain utilizes about 20% of the oxygen amount of the body, and a significant portion of that oxygen is transformed to ROS. Numerous evidence suggests that a major contributor to the dopaminergic neuronal death in PD brain are ROS, which occurs from dopamine metabolism, but also low glutathione (GSH) levels, and raised levels of iron and calcium in the SNpc. GSH is a tripeptide consisting of glutamate, cysteine, and glycine, with the reactive thiol group of its cysteine residue working as a powerful antioxidant. GSH is synthesized in the cytoplasm subsequently transported to the mitochondria, where it works as an antioxidant molecule. GSH, with the help of enzymes glutathione peroxidase (GPx) and reductase (GR), forms detoxification machinery against these oxidative species[10]. GSH levels are finely controlled in normal neurons, and alterations from the basal physiological levels can provoke cell death. The depletion during PD precedes mitochondrial and DA loss, and the degree of its damage has been seen to associate with disease severity.

Another essential mechanism implicated in the pathogenesis of PD is excitotoxicity, a pathological process during which neurons are damaged and destroyed after intense stimulation of glutamatergic receptors by glutamate, the principal excitatory neurotransmitter in the CNS. This event is implicated in several pathological conditions concerning the CNS such as stroke, epilepsy and AD. Glutamate-mediated excitotoxicity may be involved in a vicious cycle, which critically gives worsening of nigrostriatal degeneration in PD[11].

Not less severe is neuroinflammation that has been seen in postmortem brain in the form of activated microglial pro-inflammatory cytokines in SN and striatum and

has been implied as part of the pathophysiology of the disease. This inflammatory reaction is triggered by the presence of LBs because α -syn protein is an activator of microglia. The importance of activation is subordinate on the amount of the α -syn present. This can drive to the differentiation of microglia into several phenotypes, including antigen presenting or macrophage-like forms. The first one associated with lower levels of α -syn, also trigger activation of the adaptive immune system by CD4+ T-cells[11].

1.4 SYMPTOMATOLOGY

PD is a disease with a slowly progressive neurodegeneration, in which motor and non-motor symptoms occur. The disease is recognized when one of the motor symptoms develop. Motor symptoms appear when at least 50% of the dopaminergic neurons are already lost, due to the efficient compensative mechanisms of the dopaminergic system.

There are four main motor symptoms: resting tremor, bradykinesia, postural imbalance, and rigidity. Normally, the motor impairment appears on the dominant side first and gradually spread to the contralateral side, although the dominant side will be the most affected one.

- Bradykinesia is the symptom that disabling the most in this pathology and is present in 80-90% of the patients. It is characterized by slowness of the movements and causes inability to turn on the bed or to lift from a chair[12].
- Rigidity is the motor impairment that causes resistance in movements, due to the activation of agonist and antagonist muscle at the same time. This symptom is shared by 90% of the patients.

- Resting tremor is the most obvious manifestation of PD, and it is usually of the primary symptoms of the disease but on the other side the less disabling[13].
- The postural imbalance is a late motor symptom and apparently the most disabling of the previous four because cause the falling and eventually injuries. Although treatment for this symptom works at the beginning, the resistance to the drugs develops fast, presumably due to the advanced stage of the disease. Clinical data show that there are additional non-motor symptoms that may introduce the motor impairments. While the traditional therapies work directly on the motor symptoms through the dopaminergic system, the non-motor symptoms need a different clinical approach[14]. The major non-motor symptoms include cognitive abnormalities, mood, sleep, pain and sensory disorders. The importance of identifying these features in advance may increase the quality of life of patients affected by PD.

1.5 THERAPEUTIC STRATEGIES

Parkinson disease (PD) is one of the few neurodegenerative diseases with a highly effective treatment for suppressing its symptoms and signs.

In the past 50 years, levodopa (3,4-dihydroxy-L-phenylalanine) has been the leading drug for the treatment of this disease. It provides the first opportunity for clinicians to understand how the parkinsonian symptoms like resting tremor, rigidity, postural issues, are directly linked to the dopaminergic deficiency[15].

The appearance of motor complications is the main problem in the long-term control of patients with PD, in particular, the wearing-off phenomena that may cause severe impairments and decrease therapy effectiveness. Approximately 90% of patients exhibit motor impairments following 10 or more years of L-DOPA

therapy[16]. These adverse effects are quite related to the stage of the disease, dose, and duration of levodopa therapy[17]. Several trials prove that levodopa provides fewer side effects like hallucinations, somnolence, edema than dopamine agonists. However, in early Parkinson disease, dopamine agonists are more efficacious than levodopa also causing less dopaminergic motor complications, especially dyskinesia.

Several pathogenetic issues may provide motor impairments induced by L-DOPA, such as the gradual degeneration of dopaminergic neurons and the diminished chance of L-DOPA storage. In particular, alternate dopaminergic stimulation, due to L-DOPA treatment, may be linked with motor complications[18]. Recent investigations show that oxidant formation, following L-DOPA metabolism, could cause dopaminergic neuronal death[19]. The limits of L-DOPA therapy are therefore both interactions between the drug and the neuronal circuit and intrinsic drug toxicity[20].

The modern clinical approaches to limit or to delay motor impairments include preventing the start of L-DOPA therapy, the use of low-dose therapy, the administration of drugs, which exert a constant dopaminergic stimulation and the reduction of dopaminergic cell loss. The current national and international guidelines for PD therapy propose the use of L-DOPA when the disorder manifestations induce functional impairments.

Epidemiological evidence proposes that dietary antioxidants, like vitamins and polyphenols, may work as disease-modifying neuroprotective compounds, by modulation the neuronal death in both in-vitro and in vivo models[21]. Other dietary compounds, besides the well-known antioxidants, may represent treatment avenues for chronic neurodegeneration.

Sulforaphane 4-(methylsulfonyl)butyl isothiocyanate, SFN is a glucosinolate derived isothiocyanate found in cruciferous vegetables. Isothiocyanates are obtained from vegetables such as broccoli, cauliflower and Brussel sprouts and their detoxicant, and anticancer activity has been reported[22].

Recent studies have confirmed possible neuroprotective results of SFN in several neurodegenerative models. Indeed, SFN and its glucosinolate using decrease inflammation and ischemia in the CNS, this effect explains that SFN is able to cross the blood brain barrier (BBB) and prevent post-traumatic cerebral edema[23]. As with other isothiocyanates, SFN's neuroprotective mechanisms of action is not yet known.

Novel in vitro findings have revealed that continued SFN treatment protects neurons upon H₂O₂ damage and against 6-hydroxydopamine but it does not confer any outcome against another neurotoxin used as a PD model, 1 methyl-4-phenyl-1,2,3,6-tetrahydropyridine (MPTP). SFN may exert its effect by modulating the gene expression of phase II enzymes, which are recognized for their antioxidant and detoxicant action[24]. These results highlight that SFN limits the beginning phase of the neurodegenerative process, and neuroprotective results of SFN could be ascribed to the improvement of cellular antioxidant protection. The ability of SFN to directly prevent and to rescue neuronal damage has not yet been established.

Despite antioxidants and supplements could apparently assist in the treatment of PD, clinical investigations have confirmed that tocopherol, coenzyme Q10, and glutathione seem to have a poor role in the prevention or treatment of PD[25]. One of the purposes for this failure is presumably the small "therapeutic window" of direct antioxidants in patients with neurodegenerative diseases. In fact, oxidative impairment is usually substantial, and the degenerative process has already

begun at the time of the diagnosis. Consequently, antioxidants have a limited role in the area of neuroprotection and in particular in PD therapy. Hence, the difficulties of the neurodegenerative process and their complexities induced by long-term L-DOPA therapy have not yet been resolved.

2. METHODS

2.1 CELL CULTURES

Human neuronal-like SH-SY5Y were acquired from ATCC (USA). The cells were grown in Dulbecco's modified Eagle's medium (DMEM) with 10% fetal bovine serum (FBS), 2mM glutamine, 50 U/ml penicillin and 50ug/ml streptomycin. The cells were kept at 37°C in a humidified incubator with 5% CO₂.

2.2 L-DOPA

3,4-Dihydroxy-L-phenylalanine (L-DOPA) was purchased by Sigma-Aldrich. L-DOPA was freshly prepared every use. The powder was dissolved in distilled and filtered water to obtain a stock solution. The working solution was diluted directly in the culture media.

2.3 SULFORAPHANE

The Sulforaphane (SFN) was acquired from LDK (USA). The powder was dissolved in dimethylsulfoxide (DMSO) to obtain 10uM stocks. The aliquots were stored at -20°C.

2.4 DETERMINATION OF CELLS PROLIFERATION

The MTT [3-(4,5- dimethyl-2-thiazolyl)-2,5-diphenyl-2H-tetrazolium bromide] assay was used to assess the in vitro cytotoxicity of L-DOPA and SFN used in this study. SH-SY5Y cells (100 µl; 1x10⁵ cells/ml) were seeded into 96 well plates and left to adhere for 24h. The next day, the medium was removed from the wells and replaced with a medium containing L-DOPA and SFN for 24h at

37°C in 5% CO₂. After the treatment, the cells were washed with phosphate buffered saline (PBS) and then incubated with MTT (5 mg/ml) in PBS for 4h. After removal of MTT and additional washing, the formazan crystals were dissolved in isopropanol. The amount of formazan was measured (405 nm) with a multilabel plate reader (VICTORTM X, Perkin Elmer Inc., MA, USA).

2.5 APOPTOSIS ASSAY

Dual staining with fluorescent Annexin-V/propidium iodide (PI) double-staining system (Roche diagnostic GmbH, Mannheim, Germany) has been used to discriminate apoptotic and necrotic cell death, in which Annexin V-positive/PI-negative staining is regarded as apoptosis and PI-positive staining as necrosis. During apoptosis, a loss of phospholipid asymmetry leads to exposure of phosphatidylserine (PS) residues on the outer leaflet of the plasma membrane. Exposed PS residues bind the annexin V in the presence of calcium. Necrotic cells, expose PS residues but losing membrane function allow the propidium iodide (PI) to enter into the cell and bind the DNA as shown in Fig.1

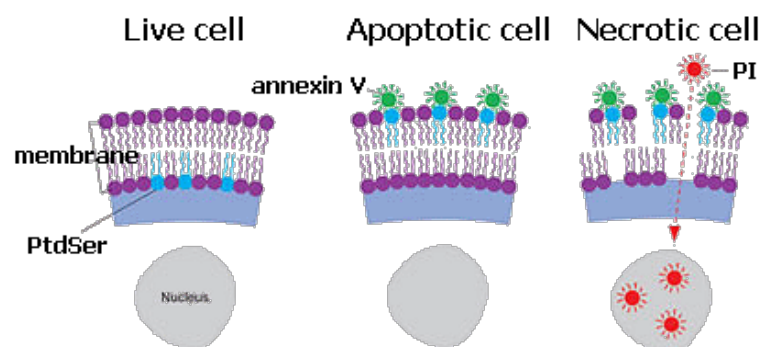


Fig.1 Representation of the labeling mechanism of cells in the presence of the Annexin-V/propidium iodide

In order to evaluate the neuroprotective effects of SFN against L-DOPA-induced neurotoxicity, an experimental approach using SH-SY5Y cells, a dopaminergic

neuronal cell line, was applied. A pulse/chase treatment has been used, which means a short exposure of neurons to L-DOPA and then it is removed to allow the activation of neuronal cell death mechanisms. In particular, apoptotic events and necrosis are detected after 15h of 3h treatment with L-DOPA, at the end of the treatment the cells were incubated with 100uL of the labeling solution at 25°C covered with aluminum foil for 15min. To evaluate the percentage of labeled cells, five random areas with about 100 cells were examined under a fluorescence microscope (Zeiss Axio Imager M1, Oberkochen, Germany). The percentage of apoptotic cells was calculated by the formula: (Annexin-V-positive cells/ n° total cells) x 100.

2.6 DETERMINATION OF INTRACELLULAR GLUTATHIONE LEVELS

The evaluation of the intracellular glutathione level was quantified through a monochlorobimane dye (MCB, Fluorescent Dyes, Los Angeles, USA). The SH-SY5Y were co-treated for 24h with a combination of L-DOPA 25uM and sulforaphane 0,63uM. At the end of the treatment, the media was removed from the wells, and the MCB 10uM was incubated with the cells for 30 mins at room temperature in the dark. The GSH levels were quantified by using a spectrofluorometer (TECAN Genios, Switzerland). The results were displayed as a fold increase versus the control.



Fig.2 representation of the chemical reaction between the MCB and GSH

2.7 ELISA ASSAY FOR ACTIVATED NRF2 TRANSCRIPTION FACTOR

The evaluation of the nuclear Nrf2 levels was collected by using TransAM[®] Nrf2 Transcription Factor ELISA Kit (Active Motif, Belgium). The Kit is composed of a 96 wells plate in which oligonucleotides containing ARE sequences (Nrf2 binding sites) are immobilized at the bottom of the wells. Active Nrf2 contained in the nuclear extracts binds the ARE sequences. A specific antibody directed against Nrf2 plus a secondary antibody conjugated to horseradish peroxidase (HRP) provides a colorimetric reaction that could be easily detected by a spectrophotometer.

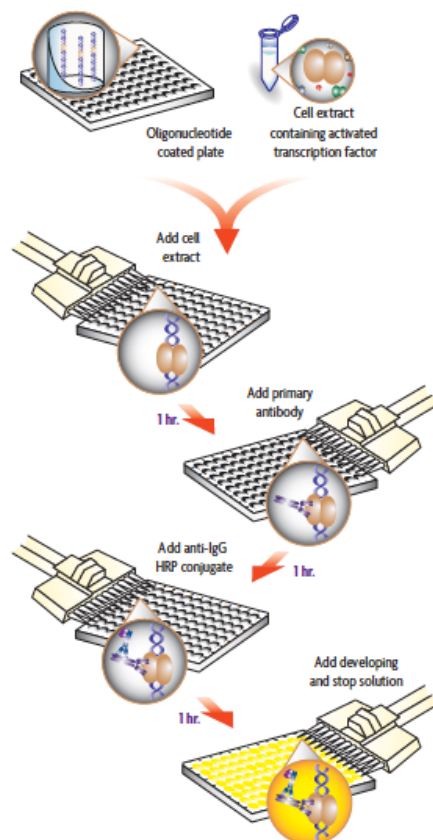


Fig.3 Representation of the main steps of the NRF2 ELISA assay

2.8 QUANTITATIVE REAL-TIME PCR

RNA was extracted from SH-SY5Y cells using the RNeasy mini kit (Qiagen) and following manufacture's procedures. cDNA was synthesized using the High capacity RNA-to-cDNA Kit (Applied Biosystem). qRT-PCR was carried out using Taqman Universal Master Mix II (Applied Biosystem) and the average mRNA fold change of each target gene was calculated by comparing the CT (cycle threshold) of the target gene to that of the housekeeping gene *18-S*. All reactions had three technical replicates and each condition had three biological replicates. The Taqman probes span an exon junction.

Relative quantification was with the $\Delta\Delta CT$ method ($2(-\Delta\Delta CT)$), and *P* values were calculated by *t*-test. The wild type was used as the calibrator to assess fold change in gene expression.

3. RESULTS

3.1 NEUROTOXIC EFFECTS OF L-DOPA

First, we evaluated the neurotoxic profile of L-DOPA in the SH-SY5Y human neuroblastoma cell line. SH-SY5Y cells were treated for 24 h with various concentrations L-DOPA (25-100 μ M). Treatment with 50 and 100 μ M of L-DOPA led to a significant increase of neurotoxicity (Fig.1).

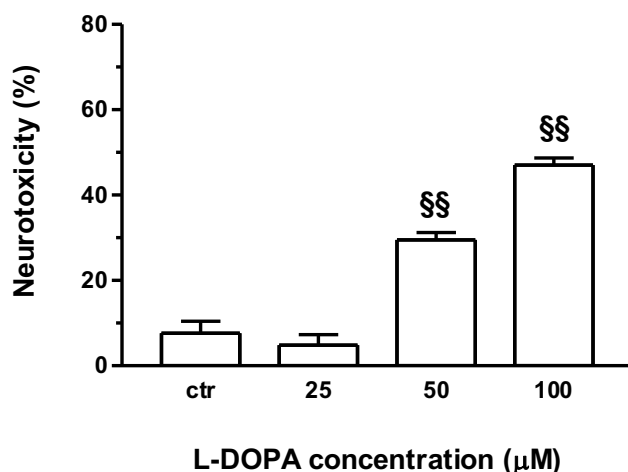


Figure 1. Neurotoxic effects of L-DOPA in SH-SY5Y cells. SH-SY5Y cells were treated for 24 h with various concentrations L-DOPA (25-100 μ M). At the end of treatment, cell viability was measured using MTT assay as described in the materials and methods section. The values are expressed as a percentage of cell viability decrease respect to untreated cells. The data shown as mean \pm SEM (n=4-5). ^{\$\$}p<0.01 vs control; at ANOVA with Dunnet post hoc test.

3.2 SULFORAPHANE COUNTERACT THE NEUROTOXICITY INDUCED BY L-DOPA

Several studies show that L-DOPA-induced neurotoxicity it may be caused by an increase of ROS, probably due to its autoxidation and metabolism. Among

indirect antioxidant molecules, isothiocyanates, derived from the glucosinolate hydrolysis found in cruciferous vegetables, have recently gained attention as potential neuroprotective compounds that induce antioxidant phase 2 enzymes and molecules through transcription factor Nrf2-dependent antioxidant response element activation. However, the potential neuroprotective effects of SFN against the neurotoxicity elicited by L-DOPA still remain unanswered. Therefore, a co-treatment with L-DOPA 100 μ M and SFN 0.63-2.5 μ M was applied on the SH-SY5Y. As showed in Fig.2, SFN counteracted the L-DOPA-induced neurotoxicity, showing a significant dose-response inhibition of the neurotoxicity with the maximum effect at 2.5 μ M.

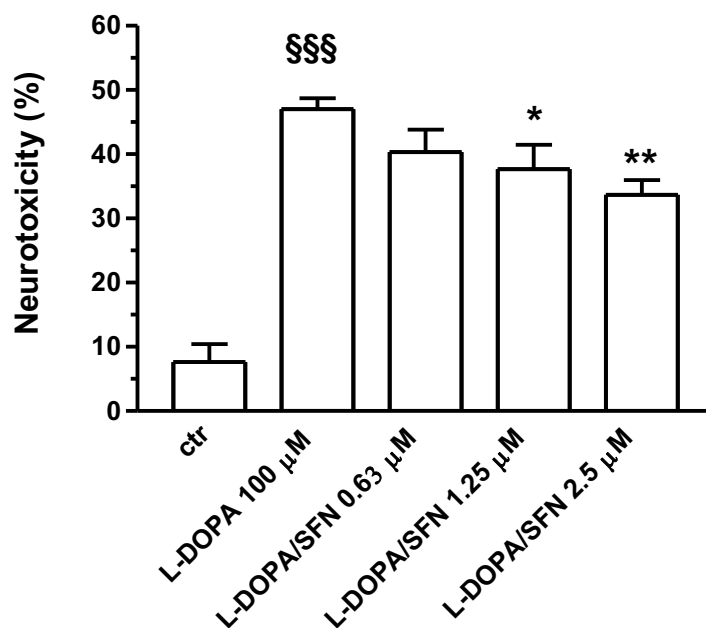


Figure 2. SFN counteracts the neurotoxicity induced by L-DOPA in SH-SY5Y cells. SH-SY5Y cells were treated with various concentrations of SFN (0.63-2.5 μ M) and L-DOPA (100 μ M) for 24 h at 37°C. At the end of treatment, cell viability was measured using MTT assay as described in the materials and methods section. The values are expressed as a percentage of cell viability decrease respect to untreated cells. The data shown as mean \pm SEM (n=4-5). §§§ p <0.001 vs control, * p <0.05 and ** p <0.01 vs cells treated with L-DOPA; at ANOVA with Dunnet post hoc test.

3.3 SULFURAPHANE PREVENTS THE NEUROTOXICITY INDUCED BY L-DOPA

Neurohormesis is the adaptive response of the organism to stress including environmental “toxins”. Many phytochemicals frequently function as toxins that defend the plants against insects and other damaging organisms. However, at the relatively low doses consumed by humans and other mammals these same “toxic” phytochemicals begin pathways that can shield the cells against a type of adverse circumstances. We evaluated the ability of the SFN to induce a neurohormetic response against a subsequent L-DOPA-induced toxicity. SH-SY5Y cells were treated with various concentrations of SFN 0.63-2.5 μM for 24 h and then treated with L-DOPA 100 μM . SFN showed a significant ability to prevent the cell death induced by L-DOPA with a neuroprotection more efficient than the co-treatment L-DOPA and SFN (Fig.3)

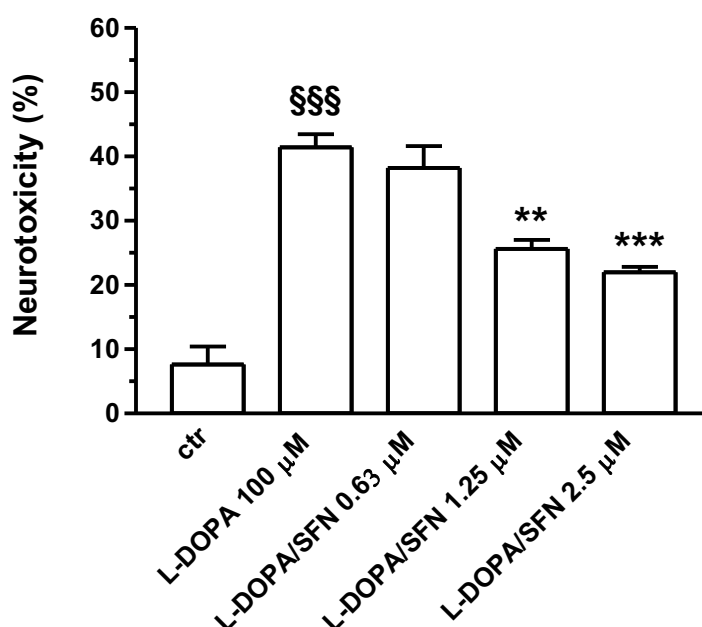


Figure 3. SFN prevents the neurotoxicity induced by L-DOPA in SH-SY5Y cells. SH-SY5Y cells were treated with various concentrations of SFN (0.63-2.5 μM) for 24 h and then treated with L-DOPA (100 μM) for 24 h at 37°C. At the end of treatment, cell viability was measured using MTT assay as described in the materials and methods section. The values are expressed as a percentage of

cell viability decrease respect to untreated cells. The data shown as mean \pm SEM ($n=4-5$). $^{\$ \$ \$}p<0.001$ vs control, $^{**}p<0.01$ and $^{***}p<0.001$ vs cells treated with L-DOPA; at ANOVA with Dunnet post hoc test.

3.4 THE COMBINATION OF SFN AND L-DOPA PREVENTS THE APOPTOSIS INDUCED BY H₂O₂

To investigate the potential therapeutic strategy based on a neurohormetic effect, a pre-treatment with L-DOPA and SFN with low and not toxic concentration was applied. SH-SY5Y cells were treated for 24 h with concentrations of L-DOPA (25 μ M) and SFN (0.63 μ M) not associated with neurotoxic and neuroprotective effects. The pre-treatment allowed the cells to activate the adaptive cellular stress response and counteract the subsequent oxidative stress elicited by 300 μ M of H₂O₂ (Fig. 4). In particular, we recorded a significant synergic effect in the combination L-DOPA and SFN with a strong reduction of the apoptosis compared with the single pre-treatments.

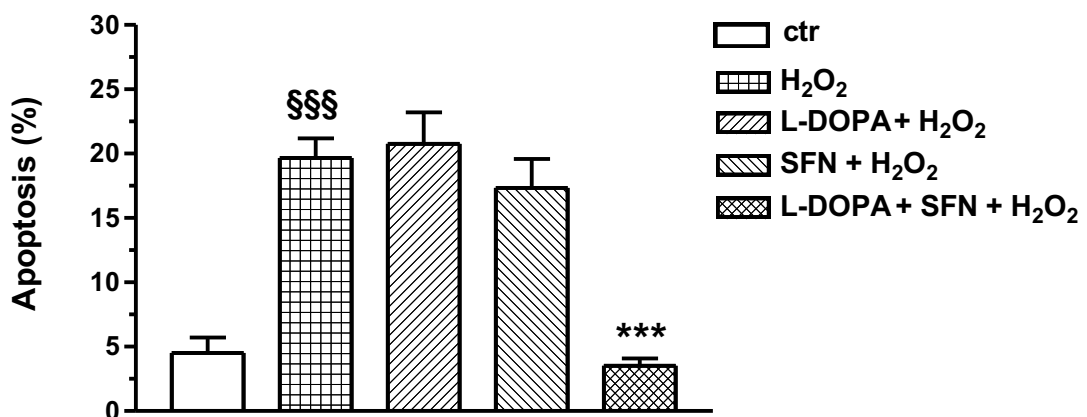
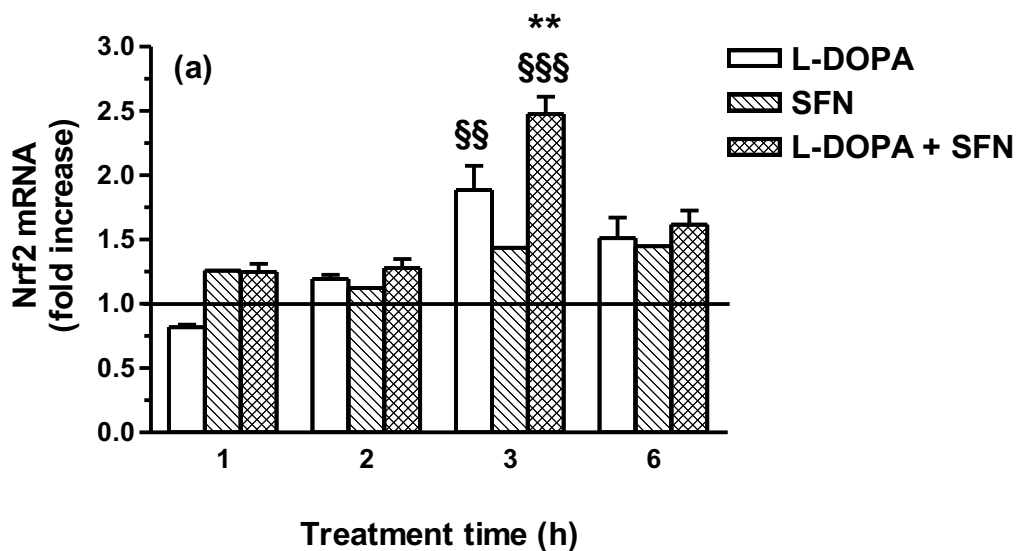


Figure 4. The combination of SFN and L-DOPA prevents the apoptosis induced by H₂O₂ in SH-SY5Y cells. SH-SY5Y cells were treated with SFN (0.63 μ M) and L-DOPA (25 μ M) for 24 h and then treated with H₂O₂ (300 μ M) for 2 h at 37°C. After a further 16 h of treatment with medium without H₂O₂, neuronal apoptosis, in terms of membrane phosphatidylserine exposure (Annexin V binding) was determined as described in the materials and methods section. The values are expressed as a percentage of Annexin V labeled neurons respect to untreated

cells. The data shown as mean \pm SEM ($n=3-4$). $§§§p < 0.001$ vs control, $***p < 0.001$ vs. cells treated with L-DOPA; at ANOVA with Bonferroni post hoc test.

3.5 SFN POTENTIATES THE INCREASE OF NRF2 mRNA AND NRF2-ARE BINDING ACTIVITY INDUCED BY L-DOPA.

The transcription factor Nrf2 is a basic leucine zipper (bZIP) protein that regulates the expression of antioxidant proteins that protect against oxidative damage. We wanted to address our findings testing the role of Nrf2 in the neuroprotection afforded by the treatments with L-DOPA 25 μ M and SFN 0.63 μ M. A kinetic treatment with different conditions was applied, and the Nrf2 mRNA level was quantified. We observed that after 3h of treatment L-DOPA was able to double the amount of mRNA of Nrf2 and that this increase is potentiated by SFN (Fig.5a). Nrf2 exerts function when is activated, migrating from the cytoplasm to the nucleus and binding ARE sequences. To evaluate the amount of Nrf2 activated, an ELISA assay was performed. Interestingly, the co-treatment L-DOPA and SFN for 2h is the only condition in which we recorded a peak of Nrf2 activated (Fig.5b).



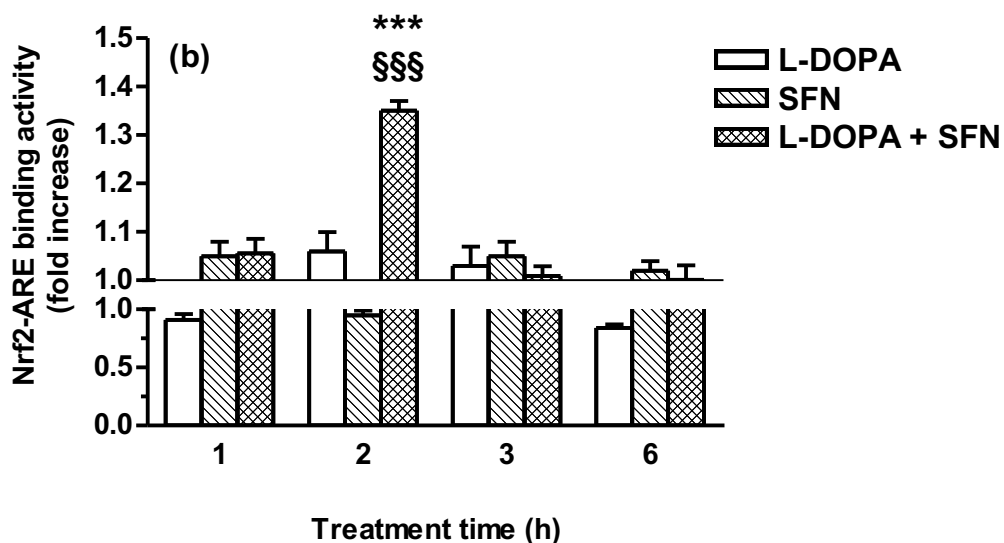


Figure 5. SFN potentiates the increase of Nrf2 mRNA (a) and Nrf2–ARE binding activity (b) induced by L-DOPA. SH-SY5Y cells were treated for different times with the combination of SFN (0.63 μ M) and L-DOPA (25 μ M) in the absence of treatment with H₂O₂. After 1-6 h of treatment, Nrf2 mRNA and Nrf2–ARE binding activity levels were measured as described in the materials and methods section. The values are expressed as fold increase respect to untreated cells. The values are shown as mean \pm SEM (n=3-4). **p<0.01 and ***p<0.001 vs cells treated with L-DOPA for the same treatment time; \$\$p<0.01 and \$\$\$p<0.001 vs cells treated with L-DOPA 1h at ANOVA with Bonferroni post hoc test.

3.6 SFN POTENTIATES THE INCREASE OF GSH INDUCED BY L-DOPA

The activation of Nrf2 results in the induction of many cytoprotective proteins. We wanted to test the level of glutathione (GSH), one of the most important downstream target of Nrf2. GSH is capable of preventing damage to important cellular components caused by reactive oxygen species such as free radicals, peroxides, lipid peroxides, and heavy metals. We treated the SH-SY5Y for 24h with L-DOPA and SFN. As shown in Fig.6, L-DOPA increase the level of GSH and the co-treatment L-DOPA and SFN potentiates the response.

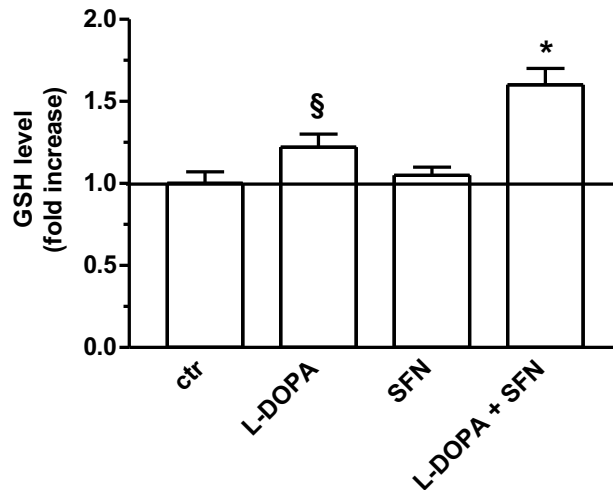


Figure 6. SFN potentiates the increase of GSH induced by L-DOPA. SH-SY5Y cells were treated for different times with the combination of SFN (0.63 μ M) and L-DOPA (25 μ M) in the absence of treatment with H₂O₂. After 24 h of treatment, GSH levels were measured using MCB as described in the materials and methods section. The values are expressed as fold increase respect to untreated cells. The values are shown as mean \pm SEM (n=3-4). §p<0.05 vs control and *p<0.05 vs cells treated with L-DOPA; at ANOVA with Bonferroni post hoc test.

4. DISCUSSION

L-DOPA is the most prescribed drug for controlling the symptoms of Parkinson's disease. However, a prolonged use of L-DOPA causes side effects like dyskinesia and gradual reduction of efficacy with the time. In order to potentiate the current treatment through the association of L-DOPA with other molecules, it is necessary to identify the cytotoxic mechanism of this drug. Neuronal death through apoptosis is hard to identify in vivo because apoptotic cells are immediately phagocytosed without generating any damage to the surrounding tissue. Because of the lacking of proof of its toxicity, it is difficult to prove that a long-term administration of L-DOPA may intensify neuronal damage and accelerate the Parkinson's progression. It has been proven that L-DOPA causes a neuronal death in vitro through apoptotic pathways mediated by an increase of ROS. Indeed, researchers found that L-DOPA toxicity was reduced in the presence of antioxidants (Walkinshaw 2016). Oxidative stress occurs when there is an impairment of the equilibrium between pro-oxidant molecules and antioxidant levels, and has been linked to the pathogenesis of several neurodegenerative diseases, ischemia, cancer, etc.

Discovering the mechanism of cell death produced by L-DOPA has significant implications for the treatment of Parkinson's disease.

This study was aimed to evaluate the antioxidant activity of SFN against L-DOPA and H₂O₂ toxicity to identify new therapeutic strategies for reducing side effects of the L-DOPA therapy. We initially identified a toxic concentration of L-DOPA (100µM) able to induce about 50% of neuronal death and found that SFN was

able to promote a significant decrease of L-DOPA-induced neurotoxicity dosage-dependent (0.63-2.5 μ M) suggesting that SFN counteracts the oxidative metabolites generate from L-DOPA. We found that co-treatment with a low dosage of L-DOPA (25 μ M) and SFN (0.63 μ M) not able to cause toxicity individually in neurons, can protect the cells from a subsequent oxidative stress induced by H₂O₂, reducing the neuronal death at the same levels of the sham. This phenomenon could be ascribed as “neurohormesis” in which some molecules at subtoxic doses activate adaptive cellular stress-response pathways in neurons. We underlined that this mechanism involves the activation of the transcription factor NRF2, known to induce antioxidant response through the activation of the transcription of several genes cytoprotective and detoxifying such as CYP1A1, GST, and NQO1.

In our work, we observed a transcriptional increase of NRF2 after 3h of treatment with the combination L-DOPA (25 μ M) and SFN (0.63 μ M) that suggests the involvement of NRF2 in the neuroprotection observed. Furthermore, we found that there is a peak after 2h of treatment of the nuclear concentration of NRF2. NRF2 in physiologic conditions is localized in the cytoplasm inhibited by its repressor Kelch like-ECH-associated protein 1 (KEAP1). Its migration to the nucleus that drives the transcription of protective genes occur under stress conditions. We hypothesize that the 2h peak of NRF2 causes an imbalance between the cytoplasmic and nuclear NRF2 that drives the increase of its transcription after 3h of treatment.

ROS in the brain tissue is counteracted by the increase in antioxidant molecules like glutathione (GSH). GSH is the main player in the detoxification against oxidative species, and its regulation is controlled by NRF2 by the regulation of

glutathione S-transferase (GST). Our findings show that SFN (0.63 μ M) potentiates the increase of GSH observed with L-DOPA (25 μ M) treatment, justifying the increase of NRF2 observed.

Taken together, these results demonstrate that SFN protects dopaminergic neurons against oxidative injury induced by high doses of L-DOPA also blocking the progression of the damage. Therefore, SFN's neuroprotective effects could not be ascribed to the induction of the synthesis of antioxidant molecules and enzymes, but they could be due to the ability of SFN to interact with specific targets of L-DOPA damage. Synergic neuroprotective effects are also very interesting, especially for the low concentrations, highlighting a high specificity in the mechanisms of action.

PART II

**KNOCK-OUT OF A MITOCHONDRIAL SIRTUIN PROTECTS
NEURONS FROM DEGENERATION IN *C. elegans***

1.INTRODUCTION

1.1 STROKE

A continuous supply of blood to the brain is essential for maintaining function and integrity. A disturbance of the blood flow can lead to stroke, in which a clot or the bursting of a blood vessel interrupts the transport of nutrients and oxygen to the brain tissue. Ischemia, caused by a clot, accounts for about 85% of all strokes, while hemorrhagic stroke accounts for about 15% [26].

Stroke is one of the leading causes of mortality in the United States and one of the leading causes of adult disability, with more than 4 million stroke survivors in the United States alone [27]. Approximately 90% of stroke survivors are left with some residual deficit, among which 30% require continued assistance and 70% are unable to resume work [28]. Gender seems to be important both in the prevalence and outcome of stroke. Not only have women been shown to have a higher risk of developing stroke, but the outcome is generally poorer than that observed in men, especially with progression of age [29].

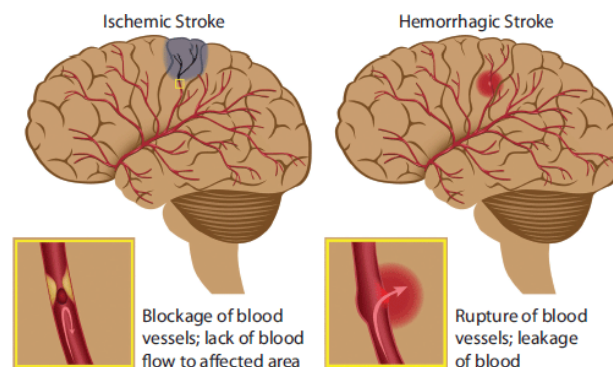


Fig.1 Ischemic and hemorrhagic strokes.

Stroke leads to massive neuronal death, in which the damage is proportional to the severity, duration, and localization of the stroke. Moreover, neuronal death

occurs differently in different brain regions depending on their distance from the blocked or burst blood vessel. Severe ischemia occurs in the central zone, referred to as the core, causing irreversible neuronal death [30]. Just outside the core, another area of the brain tissue, called penumbra is also damaged, but to a lesser extent. In the penumbra, the damage of stroke is potentially reversible [31]. For this reason, the penumbra is the main target for therapeutic intervention [30].

While stroke is a major area of medical research, effective strategies to protect against the permanent damage of neuronal death due to stroke are still not available. There are several new drugs in trial stages for the treatment of stroke. However, the plasminogen activator (tPA), which has been shown to improve outcomes in both sexes, is the only FDA-approved drug currently available [32]

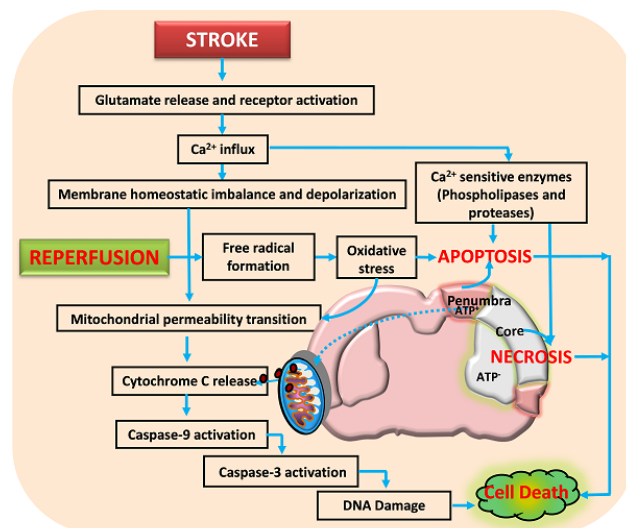


Fig.2 Stroke events. Meheta and Vemuganti, *journal.aavs*, 2014

1.2 MOLECULAR MECHANISMS OF CELL DEATH IN STROKE

The major excitatory neurotransmitter in the mammalian central nervous system (CNS) is glutamate [33]. Glutamate binds both ionotropic and metabotropic

receptors. In a physiologic condition, the activation of these receptors is well regulated. During an ischemic stroke, the level of glutamate raises to a concentration toxic to neurons [34].

The excessive calcium influx through the activation of glutamate receptors and from endoplasmic reticulum causes a dysregulation of the regulatory mechanism and leads to the activation of lipases, phosphatases, endonucleases, and calcium-dependent proteases that immediately destroy the cell and mitochondria integrity [35].

Glutamate receptors are also responsible for an excessive increase of sodium, which causes an influx of water, leading to cell swelling and edema [36]. Moreover, the increase of Na^+ , Ca^{2+} , and ADP in ischemic cells ultimately leads to an overstimulation of the mitochondrial production of reactive oxygen species, or ROS [37]. ROS directly damage lipids, proteins, carbohydrates, and nucleic acids. Inflammation also plays a crucial role in the pathogenesis of the ischemic stroke [38]. Cytokines, such as IL-1, IL-6, TNF-alpha, and TGF-beta, and adhesion molecules, such as selectins, integrins, and immunoglobulins, are involved in the inflammatory response, the beginning of which contributes to irreversible brain damage. In addition, ROS can increase inflammation directly by increasing blood brain barrier (BBB) permeability via the up-regulation of vascular endothelial growth factor (VEGF) and induction of the expression of cytokines and NF-kb. These events and reperfusion result in several types of neuronal death including, autophagy, necrosis, and apoptosis [39].

The periinfarct area surrounding an acute ischemic event is characterized by apoptosis, which has been linked to an enhanced expression of p53 [40]. p53 migrates to the mitochondria where it binds and inactivates Bcl-XL, causing cyt C

release and activation of caspase-9 [41]. Caspase-9 begins the activation of other caspases, of which caspase-6 appears to be involved in axonal degeneration. Moreover, several studies suggest the involvement of autophagy after ischemic events. The hypoxia-inducible factor (HIF) seems to be a key regulator of autophagy through the activation of autophagic genes [42].

1.3 DEG/ENaC CHANNELS TOXICITY

DEG/ENaCs channels are expressed in many organisms extending from the nematode *Caenorhabditis elegans* to mammals (ASICs). They are involved in sensory perception, such as touch sensation [43], thermosensation [44], proprioception [45] vascular and visceral mechanotransduction [46] and pain sensation [47]. DEG/ENaC channels share common characteristics and domains. They are 550-950 amino acid long transmembrane proteins, with two transmembrane helices (MSDI and MSDII), small intracellular N- and C- termini, and a significant extracellular cysteine-rich domain [48].

In *C. elegans*, the most studied DEG/ENaC is the MEC touch-transducing channel complex, which combines subunits MEC-4 and MEC10, stomatin-related MEC-2, and paraoxonase-related MEC-6 [49]; [50]. MEC-4 and MEC-10 share 48% identity, related to subunits of the ENaC channels in mammals [51]. MEC-4 is expressed only in the six touch neurons, while MEC-10 is also expressed in four other neurons (FLPs and PVDs) in which it mediates harsh touch and/or stretch sensitive response behaviors. DEG/ENaC channels can be hyperactivated either by a genetic modification, indicated by 'd', or by acidification of the extracellular environment [52].



Fig.3: The six touch sensing neurons in *C. elegans* labeled with a GFP tag.

The hyperactivation of MEC-4(d) triggers neuronal necrosis through an increase of intracellular Ca^{2+} release from the ER and activation of calpain and cathepsin proteins.

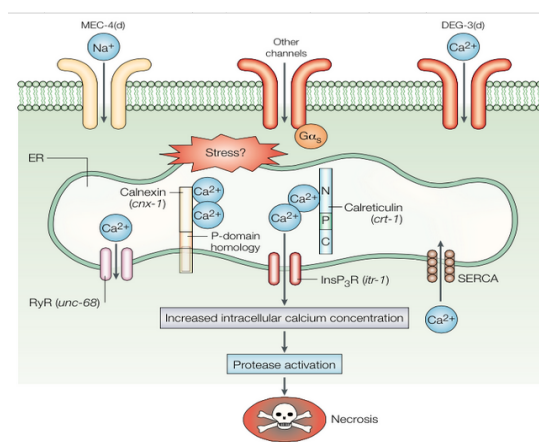


Fig.4: Neuronal death is mediated by hyperactivation of MEC-4 channel (Goodman et al., 2002).

The block of DEG/ENaC by a pharmacological approach using amiloride or by genetic mutations has been shown to protect neurons from death. In fact, point mutations that inhibit ion flux through the channel can prevent neuronal death, suggesting that the cation flux is essential for the neuronal death induced by hyperactivation of the DEG/ENaC channels.

Ca^{2+} permeability seems to be essential for the hyperactivation of these channels. Indeed, Bianchi et al. demonstrated that MEC-4(d) is Ca^{2+} permeable. Another example is the mammalian ASIC1a that results Ca^{2+} permeable under ischemic

conditions [53]. During the hyperactivation of the DEG/ENaC channels, Ca^{2+} overload that causes neuronal death is thought to derive from the extracellular compartment and the endoplasmatic reticulum [54].

Hyperactivation of the DEG/ENaC channels causes neuronal swelling and death that shows all the hallmarks of necrosis. The homeostatic mechanism that prevents cells from swelling is mediated by the Na^+ - K^+ ATPase, which pumps Na^+ outside of the cell. During and ischemic event, the oxygen and ATP deprivation leads to the block of the sodium-potassium pump, which in turn causes accumulation of Na^+ in the cells and the subsequent entry of water, leading to cell swelling. The following depolarization leads to enhanced excitability and release of neurotransmitters. Excessive glutamate release induces direct calcium entry via hyperactivated postsynaptic calcium permeable ionotropic receptors NMDA or indirectly by AMPA and kainite receptors, which activate voltage-gated calcium channels or cause sodium/calcium exchanger to operate in reverse. Calcium overload induces downstream activation of calcium-dependent enzymes that dismantle the cell.

1.4 CHEMICAL ISCHEMIA

Chemical ischemia can be used experimentally to simulate *in vitro* certain aspect of ischemic brain injury. In this model, Na^+ azide or Na^+ cyanide, inhibitors of oxidative metabolism, usually together with 2-deoxyglucose, an inhibitor of glycolysis, are utilized to induce hypoxia and hypoglycemia in cultures [55], brain slices [56], and *in vivo* [57].

These drugs block the functioning of the electron transport chain by the inhibition of the Hem groups of cytochromes in cytochrome oxidase (Complex IV). As a

consequence, redox reactions in the respiratory chain will arrest, energy will not be released, proton pumps will not work, protons will not pass through Complex V, and the production of ATP will stop.

Chemical ischemia has also been used in *C. elegans* [58]. *C. elegans* neurons, myocytes, and the whole animal are injured and killed by hypoxic exposure [58]. HIF-1 plays a central role in mammalian oxygen homeostasis and its induction has been documented under chemical ischemia condition, supporting that this model is a simple and reliable for the study of physical hypoxia.

1.5 SIRTUINS

1.5.1 MAMMALIAN SIRTUINS

Sirtuins are a group of proteins initially described as NAD⁺- dependent deacetylases [59]. The acylation of lysine is one important form of post-translational modification (PTM), comprising the addition of an acyl group to a lysine residue in proteins. This reversible modification changes the charge of the lysine residue, causing an alteration of the enzyme activity, structure, and substrate specificity of the target [60]. Because of their ability to deacetylate a wide class of protein targets, sirtuins are linked to the regulation of various cellular processes, with well-described functions in metabolism, gene transcription, differentiation, apoptosis, antioxidant resistance, and lifespan[61].

For these reasons, it is easy to understand their involvement in a large number of human diseases including neurodegenerative diseases, cancer, and metabolic diseases.

Sirtuins are phylogenetically conserved, from bacteria to mammals. Sir2 was the first sirtuin to be identified in yeast almost ten years ago, where mutants showed lifespan extension by suppressing genome instability [62, 63]. Since then, the interest of sirtuins in longevity and health-promoting effects has increased. There are seven sirtuins in mammals (SIRT1-SIRT7), all sharing a common catalytic domain and NAD⁺-binding site [64].

The deacetylase activity is exerted on different targets, such as histones, apoptotic modulators, and transcription factors [65, 66]. The fact that they depend on NAD⁺ instead of Zn²⁺ like other deacetylases, supports their dependence on the energy state of the cell. SIRT1 is the evolutionary closest member to Sir2 and, for this reason, has been the most studied of the seven sirtuins.

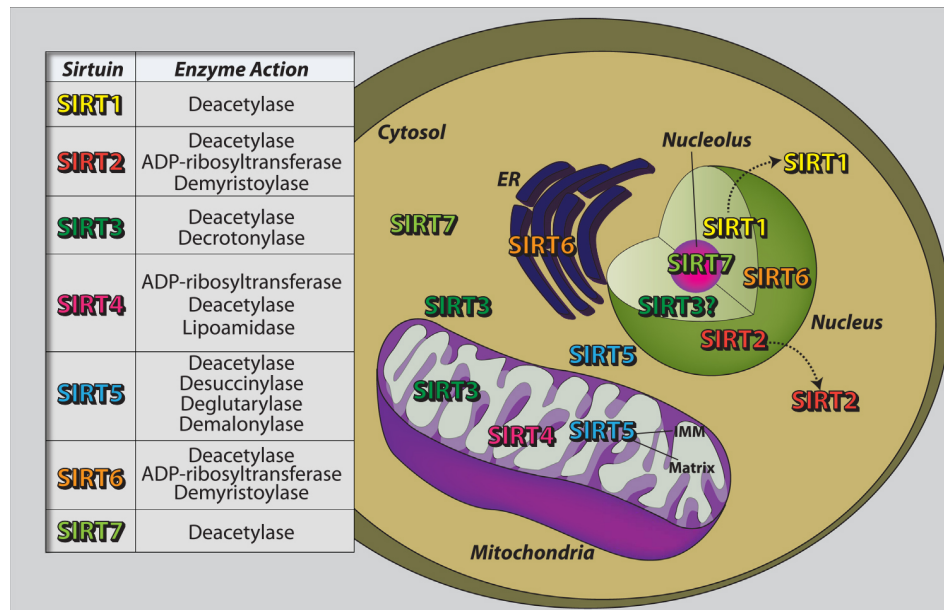


Fig.5 Human sirtuins and their functions

In addition, it has been recently shown that sirtuins catalyze other types of enzymatic reactions Fig.5, suggesting that additional sirtuins functions may still be awaiting discovery.

1.5.2 THE NUCLEAR SIRTUINS SIRT1, SIRT6, SIRT7

SIRT1

SIRT1 removes acetyl groups from lysines using NAD^+ as cofactor, forming deacetylated protein, 2-O-acetyl-ADP-ribose, and nicotinamide as a consequence. SIRT1 deacetylates and reduces the activity of central regulator proteins like p53, FOXO1, and FOXO4 [67]. Under oxidative stress, SIRT1 enhances the cell protection to stress and decreases the apoptotic capacity of FOXO3. Indeed, overexpression of SIRT1 in mice induces lifespan extension and the appearance of phenotypes correlated with delayed aging, such as improvement in terms of elevated physical activity, decrease of body temperature, oxygen consumption, and quality of sleep[68]. Conversely, repression of SIRT1 in mice abolishes the result of lifespan extension[69].

Moreover, sirtuin inhibitors, such as sirtinol, can be beneficial as therapeutic agents since up-regulated SIRT1 has been reported in cancer cell lines[70], suggesting the possibility that SIRT1 inhibition might suppress cancer cell proliferation. In addition to cancer treatment, sirtuin inhibitors have also been suggested in the treatment of Parkinson's disease[71], leishmaniasis[72], and human immunodeficiency virus[73], among others. Furthermore, increase dosage of SIRT1 *C. elegans* homolog sir-2.1 extends nematode lifespan by 50% [74] and knock-out of sir-2.1 abolishes life-extension mediated by caloric restriction [75].

Recent findings demonstrated that SIRT1 increases mitochondrial biogenesis by deacetylation of target proteins, such as peroxisome proliferator activated receptor co-activator1 α (PGC-1 α), a primary modulator of the gluconogenic pathway[76], and hypoxia-inducible factor 1 α (HIF-1 α)[77]. Overexpression of SIRT1 in liver can enhance expression of PPAR α and activate PGC-1 α , which has effects on oxidative metabolism and regulates lipid metabolism in response to

nutrients and hormonal signals. In addition, HIF-1 α and HIF-2 α bind directly to HIF-responsive elements (HREs) on the SIRT1 promoter, boosting expression of SIRT1. These studies proposed potential therapeutic advantages of SIRT1 activation for metabolic and other aging-related disorders.

SIRT6 AND SIRT7

SIRT6 and SIRT7 are nuclear proteins with a different subnuclear localization compared to SIRT1. SIRT6 is associated to heterochromatic regions, while SIRT7 is in nucleoli.

SIRT6 was reported as a mono ADP-ribosyltransferase, acting on H3K9ac and H3K56ac, preserving telomere integrity and genome stability[78]. SIRT6 knockout mice exhibit enhanced cellular sensitivity to genotoxic stress with errors in base excision repair (BER), short lifespan, and aging-like phenotypes[79]. SIRT7, on the other hand, seems to control tissue homeostasis by deacetylation of p53 and regulation of rDNA transcription[80]. Due to the similar role of SIRT1 and SIRT7 in activating p53, these two sirtuins may act together, however, this theory has not yet been proven.

1.5.3 THE CYTOPLASMIC SIRTUIN SIRT2

SIRT2 is mainly localized in the cytoplasm, but migrates to the nucleus during G2 to M transition. Many studies suggest that SIRT2 functions in regulating cell cycle progression. Overexpression of SIRT2 blocks cell cycle in starfish oocytes and SIRT2 expression is downregulated in several cancers including melanomas, gastric carcinomas, and gliomas[81]. SIRT2 mediated deacetylation of alpha-tubulin and H4K16ac before mitosis might also mediate cell cycle control. Impaired microtubule stability and altered cytoskeleton structure mediated by SIRT2-

mediated tubulin deacetylation has been linked to neuronal degeneration and interferes with oligodendrocyte differentiation[82]. SIRT2 seems to be upregulated in white adipose tissue under caloric restriction (CR) and represses adipocyte differentiation by deacetylating FOXO1. These findings propose a crucial role of this sirtuin as an energy sensor and chief regulator of metabolic pathways in response to nutrient deprivation.

1.5.4 THE MITOCHONDRIAL SIRTUINS SIRT3, SIRT4, SIRT5

SIRT3, SIRT4, SIRT5 are found in the mitochondria and play a significant role in the regulation of the PTMs in this organelle. SIRT3 is localized in the mitochondrial matrix and is the best-described mitochondrial sirtuin. One of SIRT3 targets is the Acetyl-CoA 2 (AceCS2), a key mitochondrial enzyme implicated in several pathways, including cholesterol and fatty acid synthesis[83].

SIRT4 was initially described to have NAD⁺-dependent ADP-ribosylation activity. Hagis et al. found the mitochondrial enzyme GDH to be a target of SIRT4. SIRT4, which is highly expressed in the beta cells of the pancreas, downregulates the activity of GDH, reducing mitochondrial ATP production and impairing insulin secretion[84]. While initial investigations focused on insulin secretion, later studies proposed other roles for SIRT4. The knockout of SIRT4 in mouse hepatocytes and myotubes increases the expression of fatty acid and mitochondrial metabolism genes[85]. SIRT4 was found to deacetylate malonyl-CoA decarboxylase (MCD), an enzyme that generates acetyl-CoA from malonyl-CoA. In addition to interfering with lipid catabolism, deficiency of SIRT4 has been shown to improve resistance to induction of the mPTP, influence mitochondrial uncoupling through the adenine nucleotide translocator2 (ANT2), and stimulate

enhanced entry of glutamine-derived carbon into the TCA cycle by raising GDH activity[84]. SIRT4 has also been reported to be involved in backward signaling from the mitochondria to the nucleus into an axis involving AMPK and PGC1 α . Recent studies identified new target proteins, including mitochondrial heat shock protein 60 and Stress-70, associated with cell proliferation and aging. Other publications recognized a novel role for SIRT4 as a lipoamidase enzyme. It was found that SIRT4 mediates the lipoamidation of pyruvate dehydrogenase (PDH) that leads to an inhibition of PDH activity that is an important link between glycolysis and TCA cycle.

Due to its influence on lipid and glutamine metabolism, SIRT4 has been linked to several diseases. For example, the suppression of SIRT4 may protect against type 2 diabetes. Indeed, mRNA levels in granulocytes and monocytes from normal and type 2 diabetes subjects revealed a negative association between SIRT4, plasma glucose, and high-density lipoprotein cholesterol, showing a potentially protective role of the inhibition of SIRT4 in type 2 diabetes[86]. Impairment in metabolism is also related to the development of many cancers, with genomic instability, and SIRT4 is suggested to act as a tumor suppressor. This is supported by studies showing SIRT4 KO mice to spontaneously develop various types of tumors[87].

SIRT5 is a class 3 sirtuin, present primarily in prokaryotes. It is highly expressed in tissues such as heart, skeletal muscle, brain, liver, and kidney. In SIRT5 knock-out mice, there is a little alteration of the mitochondrial acetylation state. This suggests that SIRT5 acts only in very specific targets[88]. For example, Schlicker et al. found that SIRT5 deacetylates cytochrome c, an essential protein involved in apoptosis and oxidative phosphorylation. SIRT5 also regulates the urea cycle

by deacetylating and activating carbamoyl phosphate synthetase I (CPS1) to catalyze the detoxification of ammonia[89].

The involvement of sirtuins in neuroprotection is still unclear because contradicting results support that activation or inhibition of sirtuins may be protective depending on the cellular context and type of sirtuin. For example, dietary polyphenolic compounds protect against neurodegenerative diseases via the activation of several pathways, including sirtuins[90]. Resveratrol, a phenol contained in grapes, blueberries, raspberries, and peanuts was found to protect heart and brain from ischemic injury[91] via activation of the SIRT1. Resveratrol mimics ischemic preconditioning, a technique in which the induction of short ischemic events protects against a subsequent, more potent insult. Raval et al. showed that blocking SIRT1 through the use of sirtinol eliminated the protection induced by ischemic preconditioning[92]. On the other hand, Pallos and colleagues found that reducing the level of Sir2 by 50% protected photoreceptors expressing mutant Htt in flies from death[93]. Furthermore, alpha-synuclein toxicity is prevented when SIRT2 is inhibited and treatment with sirtuinol protects cultured cortical neurons against excitotoxicity. In Alzheimer disease, down-regulation of the expression level of SIRT1 stimulates “nuclear factor kappa-light-chain-enhancer of activated B cells” (NF- κ B), which mediates inflammatory pathway and A β toxicity[94]. Finally, activation of SIRT1 by various flavonoids, such as kaempferol, quercetin, acacetin, apigenin, and luteolin, decreases neuroinflammation via NF κ B repression[95]. Moreover, it was shown that the neuroprotective or neurotoxic effect of the resveratrol depends on the concentration used as reported by Della-Morte et al[96].

1.5.5 *Caenorhabditis elegans* SIRTUINS

In *C. elegans*, there are 4 sirtuins: sir-2.1, which shares 49% of identity with SIRT1, sir-2.2 and sir-2.3, homologs of SIRT4, and sir-2.4, the homolog of SIRT6. *C. elegans* and mammalian sirtuins also share the same intracellular localization, except for sir-2.4 that is cytoplasmic instead of being nuclear (fig.7) Although *C. elegans* sir-2.2 and sir-2.3 have been suggested to function during oxidative stress[97], their role in neurodegeneration remains largely uncharacterized.

	sir-2.1	sir-2.2	sir-2.3	sir-2.4
SIRT1	49%/67%	26%/43%	23%/42%	25%/38%
SIRT2	43%/64%	26%/40%	25%/39%	24%/43%
SIRT3	45%/65%	30%/42%	26%/40%	27%/41%
SIRT4	29%/46%	50%/64%	43%/62%	23%/40%
SIRT5	33%/49%	27%/42%	28%/45%	24%/36%
SIRT6	23%/41%	23%/40%	24%/42%	37%/55%
SIRT7	27%/44%	25%/42%	25%/40%	39%/49%

Fig.6 Homologies and identities between mammalian and *C. elegans* sirtuins.

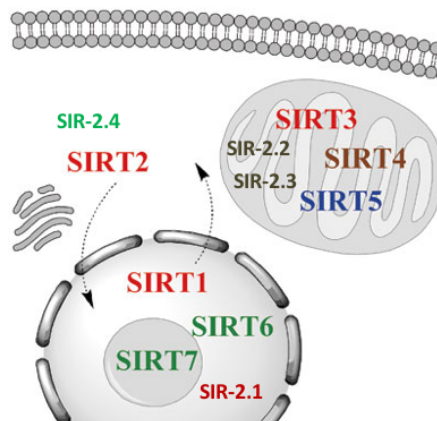


Fig.7 Cellular localization mammalian and *C.elegans* sirtuins.

The most studied *C. elegans* sirtuin is SIR-2.1. SIR-2.1 is the evolutionally closest sirtuin to mammalian SIRT1 and to the yeast SIR-2. An overexpression of sir-2.1 leads to increase the lifespan by up to 50% through the involvement of multiple

pathways that converge on the regulation of the DAF-16, a forkhead transcription factor of the FOXO family, which is negatively controlled by the insulin/IGF-1 pathway[84].

SIR-2.2 and SIR-2.3 are the homologous to the mammalian SIRT4 and are mitochondrial proteins[98]. A genome wide RNAi screen identified SIR-2.2 together with many chromatin linked factors, DNA repair/replication proteins, and cell cycle/checkpoint proteins, to be needed for genome stability in somatic and germline cells. SIR-2.2 was found to protect *C. elegans* from neurodegeneration. However, SIR-2.2 and SIR-2.3 do not appear to be involved in longevity.

1.6 CALORIC RESTRICTION

Caloric restriction (CR) is the decrease in caloric intake by about 10-50%, without compromising the right balance of essential nutrients. CR is associated with an increase of lifespan, delaying the onset of age-related diseases[99]. The theory of CR is based on the hypothesis that there is an inverse correlation between the maximum lifespan of an organism and its metabolized nutritive energy. According to this, a decrease of the metabolic rate was found to result in an increase in longevity in drosophila and *C. elegans*[100]. Since the increase of the metabolism is related to an increase in the mitochondrial function, this may be associated to an increase of ROS.

In response to food limitation or crowding, some animals are able to delay development and enter into a dormancy state known as diapause. *C. elegans* under dietary deprivation enter in a diapause state referred to as the dauer stage. *C. elegans* has been helpful in identifying signaling pathways during dauer formation. There are three main pathways involved in this phenomenon: cGMP,

TGF- β , and insulin-like signals. These act on the nuclear hormone receptor DAF-12. DAF-12, when it does not have bound insulin, triggers the development of the dauer stage through the activation of genes correlated with morphological modifications[101]. Calixto et al. showed that diapause entry inhibits neuronal degeneration. They showed that this is due to upregulation of anti-oxidative defense systems via activation of DAF-16/FOXO and SKN-1/Nrf-2. Indeed, it was found that DAF-16 activates the transcription of genes like superoxide dismutase-3 (sod-3) and Catalase-2 (ctl-1), while SKN-1/Nrf-2 activates the phase 2 detoxification enzymes[102].

Another way to induce CR is by inhibiting glycolysis. 2-Deoxy-D-glucose (2DG) is a glucose analogue that is taken up by the glucose transporters and is phosphorylated but that cannot be fully metabolized. Thus, 2-DG-6-phosphate accumulates in the cell and interferes with carbohydrate metabolism by inhibiting glycolytic enzymes. 2DG is a fully established glycolytic inhibitor which provides a physiological phenotype characteristic of CR but without notable effects on food intake. It was showed that 2DG protected fetal hippocampal cells against glutamate excitotoxicity[103]. Other studies showed that 2DG treatment could attenuate cerebral damage similar to the degree observed in CR in a model of focal ischemia. Schulz et al. showed that 2DG extends lifespan in *C. elegans*, via a mechanism dependent on AMPK signaling[104].

1.7 SIRTUINS IN CALORIC RESTRICTION

Sirtuins promote longevity and delay aging via the regulation of key proteins like p53, FOXO, and Ku70, required in either apoptotic processes or cellular repair mechanisms. Sirtuins may also slow cell death or boost the repair mechanisms of

the cell. Several studies suggest that sirtuins mediate the effects of dietary regimen and caloric restriction[105]. The expression of SIRT1 enhances upon caloric restriction in rodents and human tissues, including the liver, skeletal muscle, kidney, adipose, and brain.

The levels of NAD⁺ increase in liver cells under CR condition leading to activation of sirtuins including SIRT1. This may explain why the increases of NAD⁺ has been found to be protective for neurons. SIRT1 also activates peroxisome proliferator-activated receptor gamma coactivator 1-alpha (PGC-1 α), which results in mitochondriogenesis that may counteract malfunctioning of the mitochondrial activity that is common to many age-related diseases[106].

1.8 OXIDATIVE STRESS AND MITOHORMESIS

Mitochondria are important organelles responsible for providing energy to the cells through the generation of ATP and for producing intermediates of the Krebs cycle. Mitochondria release 90% of the ROS produced by the cell, mostly by oxidative phosphorylation. The balance between the production of ROS and its consumption must be kept in a physiologic range, as ROS are able to oxidize lipids, DNA, and proteins to cause irreversible damages. The cells prevent oxidation by ROS through antioxidant defense mechanisms that quench ROS, converting them in inert molecules[107]. Antioxidants could be divided into two categories: enzymatic and nonenzymatic. The major enzymes involved are superoxide dismutase (SODs), catalase, and glutathione peroxidase (GSH-Px). SODs are the most important because they are able to scavenge the superoxide that is the primary ROS produced by the cell. The nonenzymatic antioxidants include compounds such as vitamins C, E, beta-carotene, and GSH[108]. GSH is abundant in the cell and its ratio GSH/GSSG is the principal determinant of

oxidative stress. GSH is a cofactor for various detoxifying enzymes, such as GSH-Px and transferase. It converts vitamin C and vitamin E to their active forms. GSH production is regulated by the nuclear factor erythroid 2-related factor (Nrf2)[109].

While it is generally accepted that high levels of ROS cause damage to the cells, low levels of ROS may instead improve the cellular response to a stressor, inducing an adaptive response[107]. This dualism, in which high amounts of ROS lead to damage, versus low levels of ROS that lead to protection, is known as mitohormesis[110].

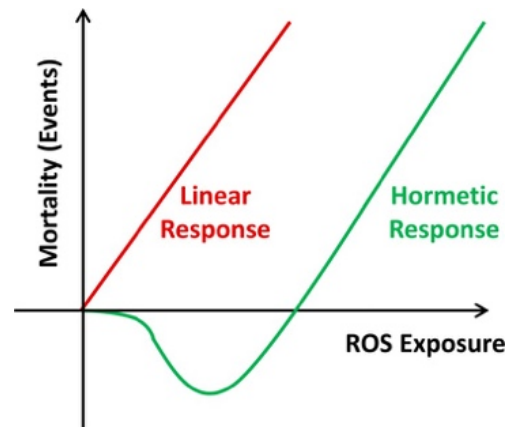


Fig.8 Mitochondrial Hormesis (Mitohormesis) (Ristow, 2014).

1.9 THE MODEL ORGANISM *Caenorhabditis elegans*

The main challenge to the identification of effective treatments starts from an inadequate understanding of the many pathways involved in diseases. Mammalian disease models offer vast similarity to the human brain, but testing the therapeutic benefit of small molecules in mammalian models is extremely costly and time-consuming. In the past decades, *C. elegans* has increasingly been used as a model system to investigate the molecular mechanisms that contribute to increased neurodegeneration[111]. Due to its well-characterized and directly available nervous system, rapid life cycle (≈ 3 days) (Fig.9) and short lifespan

(≈3 weeks), easy genetic manipulation, unique behavioral and neuropathological defects, and a surprisingly high level of biochemical conservation compared to humans, *C. elegans* is a convenient and reliable model for the study of neurodegeneration. Extraordinary similarities exist between nematode and vertebrate neurons at the molecular and cellular levels. For example, classic neurotransmitters, ion channels, receptors, [serotonin, glutamate, γ -aminobutyric acid (GABA), acetylcholine, and dopamine (DA)], vesicular transporters, and the neurotransmitter release system are related in both structure and function between vertebrates and *C. elegans*[112]. Importantly, the impact of several difficulties, such as genetic mutations or exposure to drugs on the survival and function of neuronal populations in the *C. elegans* nervous system, can be quickly investigated *in vivo*[113].

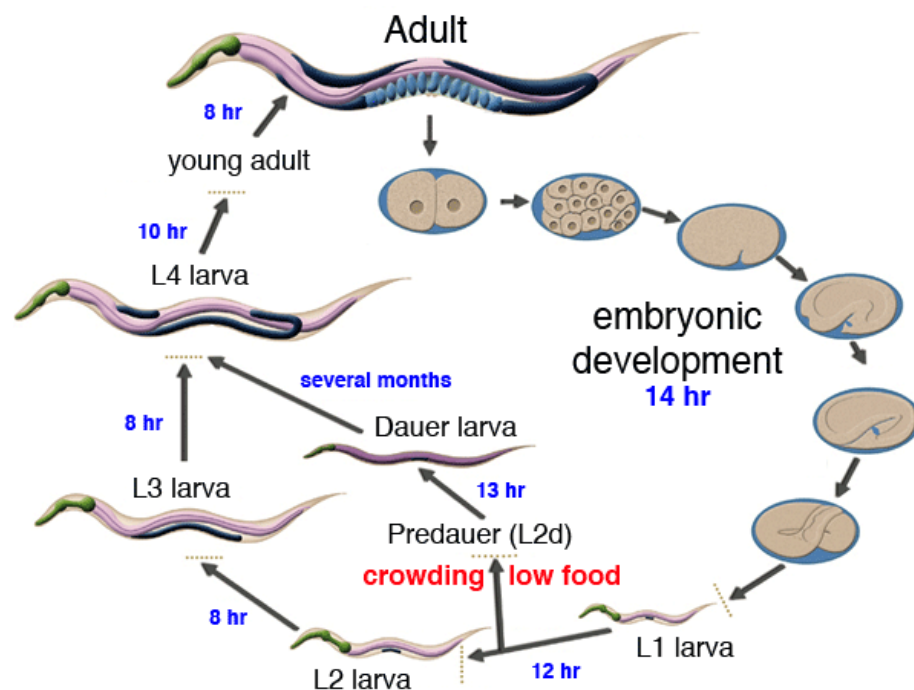


Fig.9 *C. elegans* life cycle at 22°C (artwork by Altun and Hall)

2. MATERIAL AND METHODS

2.1 CAENORHABDITIS *ELEGANS* STRAINS AND GROWTH

Nematodes were kept at 20°C on standard nematode growth medium (NMG) seeded with *Escherichia Coli* (strain OP50) (Brenner et al., 1974) as food source. For experiments with 2-deoxy-glucose (2-DG), animals were grown on plates in which 2-DG was dissolved in the agar to a final concentration of 5 mM. All animals used in this study were hermaphrodites. Males were used for crosses only. Double mutants were generated by standard crosses. Mutations were followed through the crosses by PCR and sequencing.

The following *C. elegans* strains were used in this study: Wild-type N2 Bristol, *zdl5* [*p_{mec-4}::GFP*] I to label touch neurons with GFP, VC199 (*zdl5* [*p_{mec-4}::GFP*] I; *mec-4(u231)* X), IS111 (*EX* [*MEC-10(A673T)*];*p_{mec-4}::mcherry*), RB654 (*sir-2.3(ok444)* X), BLC231 (*sir-2.3(ok444)* X ;*EX*[*zdl5* (*p_{mec-4}::GFP*) I; *mec-4(u231)* X]), BLC320 (*sir-2.1(ok434)* IV; *sir-2.3(ok444)* X; *EX*[*zdl5* (*p_{mec-4}::GFP*) I; *mec-4(u231)* X]), BLC230 (*sir-2.3(ok444)* X; *EX* [*MEC-10(A673T)*];*p_{mec-4}::mcherry*) X::*GFP*), MH1090 (*pnc-1(uk212)* IV), BLC298 (*sir-2.3(ok444)* X ;*EX*[*zdl5* (*p_{mec-4}::GFP*) I; *mec-4(u231)* X]; *EX*[*SIR-2.3*]; *unc-122::GFP*), ZB164 *bzIs8* (*p_{mec-4}mec-4::GFP*) and BCL314 (*sir-2.3(ok444)* X; *p_{mec-4}mec-4::GFP*). In *sir-2.1(ok434)* and *sir-2.3(ok444)*, 768 bp (from nucleotide 501 to nucleotide 1268) and 839 bp (from nucleotide 501 to nucleotide 1340) respectively are deleted.

2.2 MOLECULAR BIOLOGY

For the *sir-2.3* rescue construct, the 3700 bp *sir-2.3* genomic DNA sequence was amplified from N2 genomic DNA using primers

5'-GGATCCCGGAACTTCATGGCAGTGCTCTTCAAGTA-3' and 5'-

GGTACCTGACATTTCTTTCAAACATCCGAAATTCTGTAGTCTAACTTCATT-

3' that added BamHI and KpnI restriction sites to the 5' and 3' ends, respectively.

sir-2.3 genomic DNA was then cloned into pPD95.75 with the *sir-2.3* promoter.

Germline transformation by microinjection was performed as described (Mello et al., 1991).

2.3 NEMATODE SYNCHRONIZATION

Gravid adults were collected in a 1.5 ml eppendorf tubes and treated with 200 μ l of bleach and 80 μ l of 10M NaOH in 700 μ l of water for ~ 7 min to release the eggs. After centrifugation for 3 min at 3000 rpm and removal of the supernatant, eggs were resuspended in 100 μ l of sterile water, prior to inoculation onto seeded NGM plates.

2.4 FLUORESCENT MICROSCOPY

Animals were mounted on thin agarose pads and immobilized by 20 mM Na-azide. Fluorescent micrographs were taken using a LEICA DMR2 fluorescent microscope equipped with 40X and 63X objective, a Spot RT slider camera (Diagnostic Instruments) equipped with Spot32 acquisition software, a LEICA green fluorescent protein (GFP) plus filter (460/480 nm excitation filter) and a LEICA rhodamine filter (535/550 nm excitation filter). For strict quantitative

comparisons, images were acquired using the same exposure time; images were analyzed and processed using ImageJ.

2.5 CHEMICALLY INDUCED ISCHEMIA AND QUANTIFICATION OF NEURONAL DEATH

For chemical induced ischemia, synchronized adult worms were exposed for 5h at 22°C to the following solutions: 1) S Basal at pH 6.5 (for 100 ml of solution: 0.584 g NaCl, 0.1 g K₂HPO₄, 0.6 g KH₂PO₄, Acetic Acid 57 µl); 2) S Basal at pH 6.5 plus 100 mM Sodium Azide. After treatment, worms were allowed to recover onto fresh NGM plates for 20 hours at 20°C and then stained with DiD (Swanson RA et al.,1997, Scott BA at al., 2002). Animals were visualized under a 40X objective using rhodamine filters and DiD stained amphid sensory neurons were counted in each animal.

For quantification of neuronal death in *mec-4(d)* and *mec-10(d)* strains, GFP or mcherry expressing touch neurons were counted in synchronized L4-staged animals, and swollen PLM touch neurons were counted in synchronized L1-staged animals.

2.6 CAENORHABDITIS *ELEGANS* EMBRYONIC CELL CULTURE

Embryonic cell culture was performed as described previously (Sangaletti and Bianchi, 2013). Briefly, a large number of gravid adult worms were grown on enriched peptone agar plates (8P) with NA22 *Escherichia Coli*, collected in 50 ml tubes, washed 3 times with sterile H₂O and centrifuged at 1200 rpm for 10 minutes. After removal of the supernatant, nematodes were transferred into 15 ml tubes and lysed with 5-6 ml of lysing solution (5 ml of fresh bleach, 1.25 ml of 10N

NaOH and 18.5 ml of sterile H₂O) for 5-10 min. The lysis was stopped by adding egg buffer (118 mM NaCl, 48 mM KCl, 2 mM CaCl₂, 2 mM MgCl₂, 25 mM Hepes, pH 7.3, 340 mOsm) to the tube. Lysed animals were then centrifuged for 10 minutes at 1,200 rpm. Eggs were separated from the animal carcasses using 2 ml of egg buffer plus 2 ml of 60% sucrose and centrifuged for 20 min at 1,200 rpm. Eggs floating at the top of the tube were collected in a new 15 ml tube with a P1000 pipetor, washed 3 times with fresh egg buffer and centrifuged for 10 min at 1,200 rpm. To dissociate the embryonic cells, eggs were incubated for 10-30 minutes with 1 ml of 2 mg/ml Chitinase (Chitinase from *Streptomyces Griseus*-Sigma Aldrich, C6137-25UN) dissolved in egg buffer pH 6.5. After enzymatic treatment, embryos were pelleted by centrifugation for 3 min at 2,500 rpm. The supernatant was removed and the eggs were resuspended in L-15 medium (L-15 culture medium from Gibco, 10% Fetal Bovine Serum, 45 mOsm Sucrose, 1 U/ml Penicillin and 100 µg/ml Streptomycin). Cells were manually dissociated using a 10 ml syringe equipped with a 18 Gauge needle. The suspension containing cells and debris was subsequently filtered using a sterile 5 µm Millipore filter. Filtered cells were pelleted for 3 min at 2,500 rpm and resuspended in fresh L-15 medium. Cells were plated at ~230,000 cell/cm² density in 24 wells plates on microscope slides (12 mm diameter) previously coated with 0.5 mg/ml peanut lectin (Sigma Aldrich, L0881-10MG). The media was replaced the day after and the cells were kept at 20°C for up to 7-9 days. To quantify the number of GFP touch neurons alive cells were fixed using the following protocol: the medium was removed and cells were washed three times with physiological solution (145 mM NaCl, 5 mM KCl, 1 mM CaCl₂, 5 mM MgCl₂, 10 mM Hepes, 20 mM D-glucose, 25 mM sucrose, pH 7.2, and 345 mosmol/kgH₂O). Cells were then fixed for 15 min with 4% paraformaldehyde dissolved in physiological solution and washed three times with

egg buffer. Coverslips were mounting using Vectashield mounting medium and photographed using a 63X oil objective and GFP filter as described above.

2.7 QUANTITATIVE REAL-TIME PCR

RNA was extracted from synchronized young adult worms using TRIzol reagent (Invitrogen), following manufacturer's procedures, after 5 washes with sterile water. cDNA was synthesized using the High capacity RNA-to-cDNA Kit (Applied Biosystem). qRT-PCR was carried out using Taqman Universal Master Mix II (Applied Biosystem) and the average mRNA fold change of each target gene was calculated by comparing the CT (cycle threshold) of the target gene to that of the housekeeping gene *pmp-3*. All reactions had three technical replicates and each condition had three biological replicates.

The Taqman probes span an exon junction: *sir-2.1* (3-4, 3-5), *sir-2.2* (5-6), *sir-2.3* (5-6), *sir-2.4* (2-3), *pmp-3* (3-4, 4-5). Relative quantification was with the $\Delta\Delta CT$ method ($2^{-\Delta\Delta CT}$), and *P* values were calculated by *t* test. The wild type was used as the calibrator to assess fold change in gene expression.

2.8 QUANTIFICATION OF ROS

ROS levels were quantified in WT (N2) and RB654 *sir-2.3(ok444)*. Adult *C. elegans* nematodes were divided into two groups: starved for 48h in absence of food and fed with *Escherichia Coli* (strain OP50⁻). The animals were incubated with 50 μ M H₂-DCFDA (Sigma-Aldrich) for 1h under shaking condition at room temperature. The working solution 100 μ M in M9 was made from a 50mM stock solution in DMSO. The fluorescence of each worm was measured through a fluorescent microscope LEICA DMR2 at Ex/Em 495/527 nm after immobilization

of the worms with NaAzide 20mM with the same exposure time (800ms). The analysis of the intensity of the fluorescence was performed with ImageJ.

2.9 SAMPLE SIZE AND DATA REPLICATION

In Figure 1, 300 adult animals were used for panel C-F. N of experiments was 1 for panel C and D, 3 for panel E and 1 for panel F. Each RT-PCR experiment was replicated 3 times. In panel G N=50 adult animals analyzed for each condition. The experiment was replicated 4 times in the laboratory. In Figure 2 panel A-D, N was 23 experiments for *mec-4(d)* and *mec-4(d);sir-2.3* and 4 for *mec-4(d);sir-2.3;SIR-2.3*. 50 animals per strain were analyzed in each experiment. Panel E-H N=4 experiments, using at least 50 animals per strain in each experiment. Panel J number of experiments was 5 for *mec-4(d)* and *mec-4(d);sir-2.3(ok444)* and 4 for *mec-4(d);sir-2.3(ok444);SIR-2.3*. 50 animals per strain were analyzed in each experiment. In Figure 3 number of animals for wild-type were 24 and 25, for *pnc-1(ku212)* mutant were 23 and 25 in control condition and azide respectively. The experiment was replicated 3 times. In Figure 4, panel A-D number of animals was 30 in each experiment and condition. The experiment was replicated 4 times. In Figure 5 panel G, N=2 coverslips per each strain (wild-type, *mec-4(d)* and *mec-4(d);sir-2.3(ok444)*) and condition (control and 10 mM 2-DG). 10 fields were scored for each coverslip. The experiment was repeated 5 times. Panel H N=2 coverslips per each strain and condition (See detail in Figure legends section). 10 fields were scored for each coverslip. In Figure 6 panel A, number of animals was (from left to right) 22, 55, 23, 68, 25, 23, 23, 16, 38 and 35 obtained from 12 experiments. In Suppl. Figure 1 panel A, N= 300 adult animals. The experiment was replicated 3 times. Panel B, N=3 experiments using at least 30 animals for

each strain. Suppl. Figure 2 Panel C N= 30 animals for each strain. The experiment was replicated 3 times.

2.10 STATISTICS

We used Origin version 6.1 and 9 for calculation of statistical analysis. Differences between two groups were assessed using two-sample t-Test. Anova with Bonferroni's multiple comparison test was used to compare more the two groups. All p-values <0.05 were considered significant. Statistical analysis and P values are listed in detail at the end of each figure legends.

3. RESULTS

3.1 LONG LASTING PROTECTION OF DIAPAUSE AGAINST *mec-4(d)* AND *mec-10(d)* INDUCED NEURONAL DEATH

MEC-4 and MEC-10 are DEG/ENaC proteins that form the pore of the channel complex. Mec-10 is 53% identical to *mec-4* with which it coassemble to form a heteromultimeric channel complex in *C. elegans* touch neurons [114]. *Mec-4(d)* is a mutation that causes a dramatic death of *C. elegans* touch neurons by hyperactivation of Na⁺/Ca²⁺ channel MEC-4 (*mec-4(d)*). *Mec-10(d)* is a mutation that causes only a mild degeneration when hyperactivated. While *mec-4* is the main channel subunit, *mec-10* functions as a modulatory subunit [114-117]. There are six touch neurons in *C. elegans*: two anterior lateral microtubule cells (ALMs), one anterior ventral microtubule cell (AVM), two posterior lateral microtubule cells (PLMs) and one posterior ventral microtubule cell (PVM).

We quantified the extent of neurodegeneration counting the number of surviving GFP-expressing touch neurons in L4 larval stage in transgenic lines labeled by GFP (*Pmec-4::GFP*) in which the GFP is expressed only in the touch neurons.

We found that at the L4 larval stage 0.36 +/- 0.02 ratio of the *mec-4(d)* animals have no surviving touch neurons, 0.38 +/- 0.02 ratio have one surviving touch neuron and 0.24 +/- 0.03 ratio have 2 surviving touch neurons which in most cases are AVM and PVM (Fig. 1 A-E).

Calixto and colleagues showed that diapause entry called dauer state, in *C. elegans* protects touch neurons against *mec-4(d)* induced neuronal death and that the protective effect lasts for hours after exit from the dauer state [102].

We confirmed these results by finding that 16 hours after dauer exit, the ratio of L4 animals with 0 surviving touch neurons is 0.08 +/- 0.02, the ratio with 1 surviving touch neurons is 0.31 +/- 0.04 and the ratio with 2 surviving touch neurons is 0.45 +/- 0.03. In 0.14 +/- 0.04 ratio of animals that have spent time in diapause, we found 3 surviving touch neurons (an ALM or a PLM, rarely 2 ALMs or 2 PLMs), which we never observed in *mec-4(d)* L4 animals grown in the presence of food (Fig. 1 A-E).

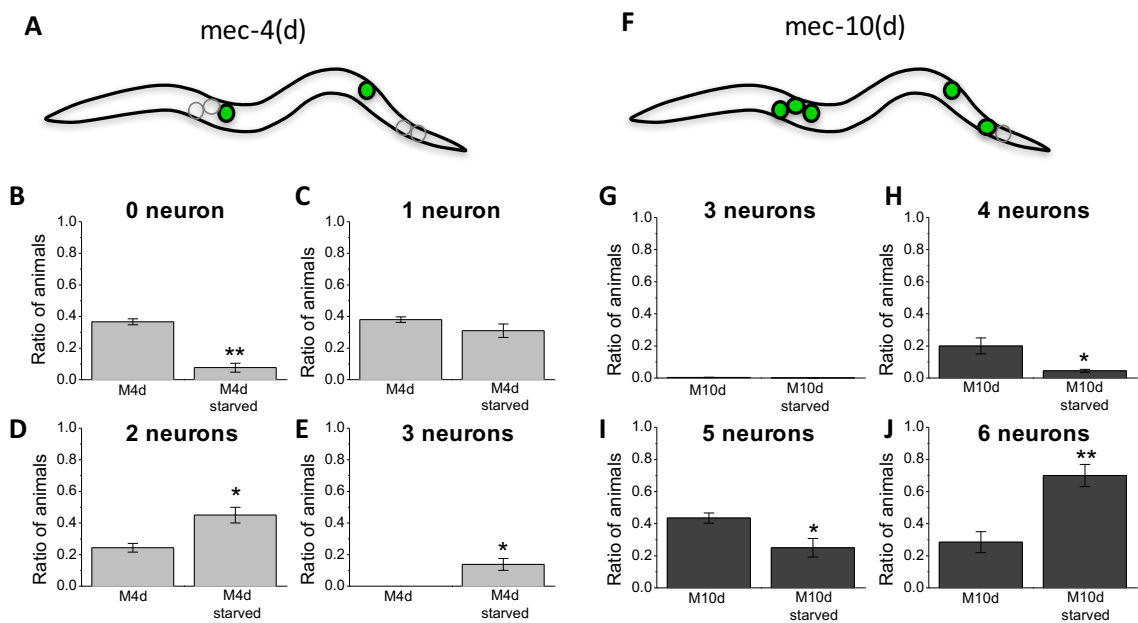


Fig. 1. Having been in dauer state is protective against *mec-4(d)* and *mec-10(d)*-induced neuronal death. **A:** Schematic drawing of a *C. elegans* with the location of the 6 touch neurons that express *mec-4* (2 ALMs, AVM, 2 PLMs and PVM). In *mec-4(d)*, the two neurons that usually survive are AVM and PVM (shown in green). **B-E:** Ratio of *mec-4(d)* animals continuously grown in the presence of food and recovered from the dauer state (labeled a “starved”) that have either no surviving, or 1, 2 or 3 surviving touch neurons. N of experiments was 3 and 5 respectively, with at least 50 animals analyzed per experiment. **F:** *mec-4* homologous subunit *mec-10* is expressed in touch neurons also. Shown in green are the neurons that survive in animals that express the transgene of the hyperactive mutant *mec-10(d)*. **G-J:** same as in B-E for *mec-10(d)* expressing animals. N of experiments was 4 for both, with at least 50 animals analyzed per experiment. Data are expressed as mean +/- SE. * and ** indicate $P \leq 0.05$ and 0.01 respectively by Student’s t-test.

To test whether the protective effect afforded by diapause entry is more robust under less toxic conditions, we compared the extent of touch neurons degeneration in animals expressing *mec-10(d)* transgene grown under control

conditions and 16 hours after dauer exit. In line with its modulatory role in channel function, *mec-10* causes only mild degeneration when hyperactivated by mutation A673T corresponding to A713V/T in *mec-4* [114, 116]. We found that diapause was protective in *mec-10(d)* induced neuronal death to a similar extent as it is protective in *mec-4(d)* (Fig. 1 F-J). Indeed, the ratio of L4 animals with 4, 5 and 6 surviving touch neurons is 0.20 +/- 0.05 and 0.02 +/- 0.01, 0.43 +/- 0.03 and 0.25 +/- 0.06, and 0.28 +/- 0.06 and 0.70 +/- 0.07 for animals grown under standard conditions and animals recovered from dauer respectively. These results are in line with the results reported by Calixto and colleagues [102] and show that cellular/organismal protective modifications that occur when the animal enters into diapause are maintained for at least 16 hours after dauer exit. These data also show that comparable effects mediated by entry in diapause are present under both strong and mild toxic insults [118].

3.2 KNOCK-OUT OF A MITOCHONDRIAL SIRTUIN IS PROTECTIVE AGAINST NEURONAL DEATH

Sirtuins are NAD⁺-dependent deacetylases and mono-ADP-ribosyltransferases that link nutrient availability/cellular metabolism to aging, cancer growth and neurodegeneration Qin, 2006 [63, 119-123]. We thus, hypothesized that sirtuins might be involved in the protective effect mediated by diapause. To test this hypothesis, we first wanted to establish whether the mRNA of sirtuins is regulated in conditions that promote neuronal death. To this end, we established a protocol to induce ischemia in the whole animal, from which we then extracted mRNA to perform real time RT-PCR experiments.

Chemical ischemia was induced by incubation of *C. elegans* in 100 mM azide at pH 6.5, followed by a recovery period [58, 124]. Azide blocks complex IV of the electrontransport chain, blocking ATP production and consequently causing cell death by necrosis [125]. To confirm that this protocol was effective in inducing neuronal death, we stained treated animals with the lipophilic dye DiD. DiD is taken up by neurons that are exposed to the outside environment, including amphid sensory neurons.

There are 12 amphid sensory neurons, 11 of which are chemosensory neurons (ADF, ADL, ASE, ASG, ASH, ASI, ASJ, ASK, AWA, AWB, AWC) which *C.elegans* use to sense chemicals. The twelfth, AFD, is a thermosensory amphid neuron. As a result of what these tiny animals sense, they can either decide to move toward the chemical (as with chemical attractants), away from the chemical (as with chemical repellants), or not at all (Bargmann CI 2006).

The uptake of the fluorescent dye requires retrograde transport and therefore it does not occur in dead or sick neurons [126]. In animals incubated in buffer at pH 6.5, all 12 amphid sensory neurons are stained with DiD (Fig. 2A). Conversely, in animals treated with azide an average of 1 amphid sensory neuron per animal is stained (Fig. 2B), confirming that this treatment causes neuronal demise and likely the demise of other cells in the animal. Importantly, we found that also in this model limiting dietary deprivation protects against neuronal death, as many more amphid sensory neurons survive azide treatment in animals that have been in diapause.

To test the effect of chemical ischemia on the transcription of sirtuin genes, we extracted mRNA from the treated animals every hour for the length of the 5 hours

treatment and performed real time RT-PCR. We found that while the mRNAs of sir-2.1 and sir-2.4 were relatively stable during azide treatment, the mRNA of sir-2.2 has a peak of transcription after 2 hours of treatment and the mRNA of sir-2.3 is elevated throughout the 5 hours of azide treatment, reaching about twice the amount after 5 hours (Fig. 2 C-F). Both sir-2.2 and sir-2.3 are localized in mitochondria and share the highest similarity with mammalian mitochondrial SIRT4 (50% and 42% identity, and 64% and 63% similarity, respectively) [85]. Given that the mRNA of sir-2.3 is elevated throughout the azide treatment, we focused on this sirtuin and wondered whether sir-2.3 might be involved in cell death induced by azide treatment. To test this possibility, we acquired sir-2.3 knock-out mutants (sir-2.3(ok444)) [85] and quantified amphid sensory neurons DiD uptake in these animals following azide treatment. Surprisingly, we found that a significantly higher number of amphid sensory neurons survived in sir-2.3 knock-out mutants versus wild type (3.36 +/- 0.87 and 0.74 +/- 0.21 for sir-2.3 and wild type respectively) (Fig. 2 G). The protective effect of knock-out of sir-2.3 likely extends to other cells in the animal as fewer sir-2.3 animals die when treated with azide (0.65 +/- 0.08 ratio of wild type animals die, 0.33 +/- 0.12 ** of sir-2.3 knock-outs, and 0.57 +/- 0.07 for sir-2.3; SIR-2.3 rescue animals, 3 experiments with at least 50 animals per experiment, ** indicates $p \leq 0.01$ by ANOVA with Bonferroni correction). To confirm that the effects of sir-2.3 knock-out is mediated by the lack of this gene, we quantified amphid sensory neurons DiD uptake in rescue animals in which sir-2.3 was reintroduced under the control of its own promoter in the sir-2.3 knock-out background. As expected for a gene specific effect, the number of amphid sensory neurons that are stained is restored to typical levels found in wild type background in sir-2.3;SIR-2.3 animals.

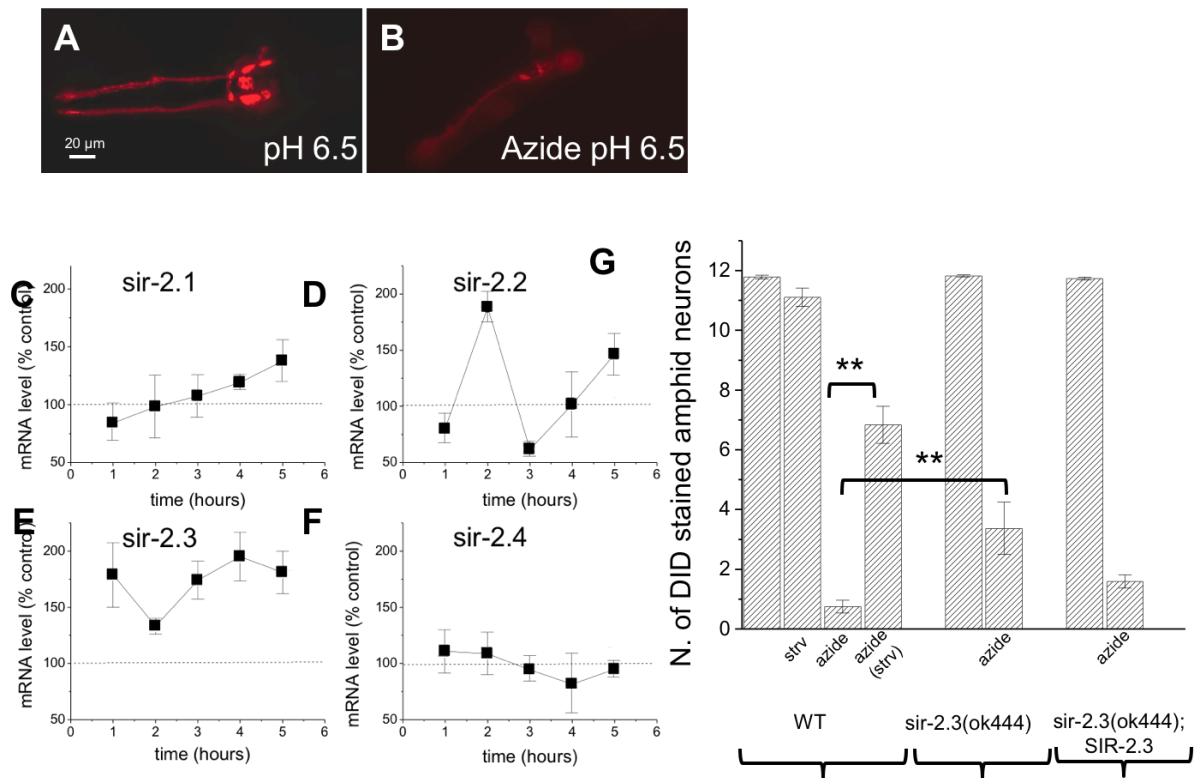


Fig. 2. The messenger RNA of mitochondrial SIR-2.3 is elevated and its knock-out is protective in a model of hypoxic ischemia. **A:** Photograph of the head of a wild type *C. elegans* incubated in S Basal at pH 6.5 for 5 hours and stained with the lipophilic dye DiD. DiD is taken up by 6 pairs of amphid sensory neurons (ASKs, ADLs, ASIs, ASHs, ASJs, and AWBs) exposed to the outside environment. **B:** Photograph of an animal treated with 100 mM azide at pH 6.5 for 5 hours and stained with DiD. Fewer stained sensory neurons are visible in this animal as a result of neuronal death. Scale bar is 20 μ m. **C-F:** Relative (compared to *pmp-3* housekeeping gene) abundance of mRNA of the 4 *C. elegans* sirtuins in animals treated for 5 hours with 100 mM azide. N of experiments was 1 for sir-2.1, 1 for sir-2.2, 3 for sir-2.3 and 1 for sir-2.4. In each experiment RT-PCR was done in triplicate. **G:** Number DiD stained amphid sensory neurons in wild type, wild type under dietary deprivation (DD), *sir-2.3* knock-out animals and *sir-2.3*;SIR-2.3 rescue animals incubated for 5 hours in S Basal at pH 6.5 and in S Basal at pH 6.5 containing 100 mM Na-azide. The number of experiments was 4 with at least 50 animals analyzed per experiment. Data are expressed as mean \pm SE. P were 0.01 and 0.0015 by ANOVA with Bonferroni correction.

Given the documented role of sirtuins in providing protection against ageing and degenerative diseases, we wondered whether the knock-out of sir-2.3 causes compensatory increase of expression of another sirtuin gene, which in turn would provide protection against neuronal death. To test this possibility, we performed real time RT-PCR on mRNA extracted from sir-2.3(ok444) mutants. We found no change in mRNA level for the other 3 sirtuins (Fig. 3).

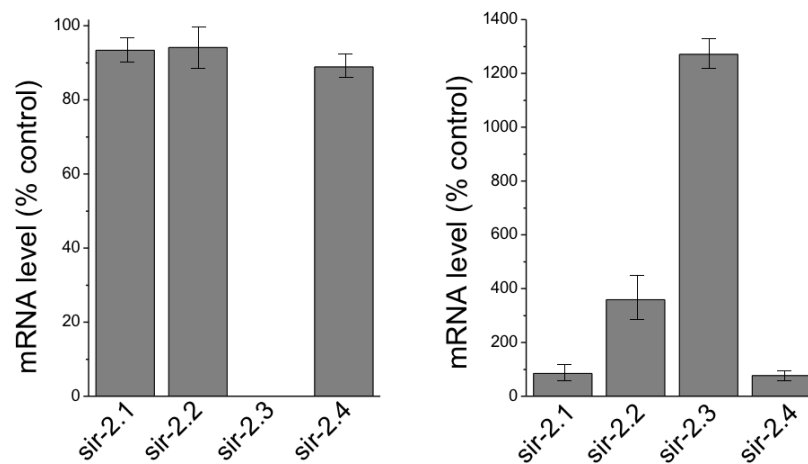


Fig. 3: Sirtuins mRNA in *sir-2.3* knock-out (A) and *sir-2.3*;SIR-2.3 rescue strains (B): Quantitative real-time PCR (qRT-PCR) from total RNA in *sir-2.3* strain was conducted using Taqman gene expression assays in order to quantify the levels of mRNA for sirtuin genes. mRNA percentage of each target gene was calculated by comparing the CT (cycle threshold) of the target gene to that of the housekeeping gene *pmp-3*. The wild-type N2 (Bristol) strain was used as the calibrator. All conditions had three technical replicates.

Furthermore, in *sir-2.3*;SIR-2.3 rescue animals, the mRNA of *sir-2.3* is overexpressed as expected for a non-integrated transgenic *C. elegans* strain, yet there is no change in the extent of neuronal death, even for shorter incubation times with azide which cause less cell death, suggesting that over expression of this mitochondrial sirtuin does not provide protection. A similar conclusion can be drawn in the case of *sir-2.2* whose mRNA is also elevated in *sir-2.3*;SIR-2.3 animals.

To conclude these data suggest that knock-out of mitochondrial sirtuin *sir-2.3* in *C. elegans* is protective against cell death caused by chemical ischemia, a surprising result given that activation of sirtuins has been previously suggested to provide protection against ageing and degenerative conditions [62, 63, 119-122].

3.3 KNOCK-OUT OF sir-2.3 IS PROTECTIVE IN HYPERACTIVE MEC CHANNEL INDUCED NEURONAL DEATH

mec-4(d) and mec-10(d)-induced touch neurons degeneration shows all the hallmarks of necrotic cell death including elevation of intracellular Ca^{2+} and activation of Ca^{2+} -sensitive calpains and cathepsins [54, 116, 127, 128]. We thus reasoned that knock-out of sir-2.3 might be protective in hyperactive mec channel induced cell death as well. To test this prediction, we crossed sir-2.3 knock-out with mec-4(d) and mec-10(d) strains and quantified touch neurons degeneration in L4 larvae. Consistent with the results in animals treated with azide (Fig. 2 G), more touch neurons survive in sir-2.3 knock-out animals than they do in animals in which sir-2.3 gene is wild type, when either mec-4 or mec-10 are hyperactivated [49, 116]. More specifically, the ratio of mec-4(d) animals that have no surviving and 2 surviving touch neurons went from 0.27 +/- 0.03 and 0.25 +/- 0.02, to 0.12 +/- 0.01 and 0.43 +/- 0.03 in sir-2.3 knock-out animals (ratio of animals with 1 surviving touch neuron remained unchanged). The effect is gene-specific, as the extent of neuronal death is restored to control levels in mec-4(d);sir-2.3;SIR-2.3 rescue strain (ratio of animals with 0 and 2 surviving touch neurons was 0.24 +/- 0.05 and 0.22 +/- 0.06 respectively, Fig. 4 A-D). Similarly, the ratio of mec-10(d) animals that have 4 and 6 surviving touch neurons went from 0.20 +/- 0.05 and 0.28 +/- 0.06, to 0.01 +/- 0.01 and 0.65 +/- 0.03 in sir-2.3 knock-out animals (no change was observed in the ratio of animals with 5 surviving touch neurons) (Fig. 4 E-H).

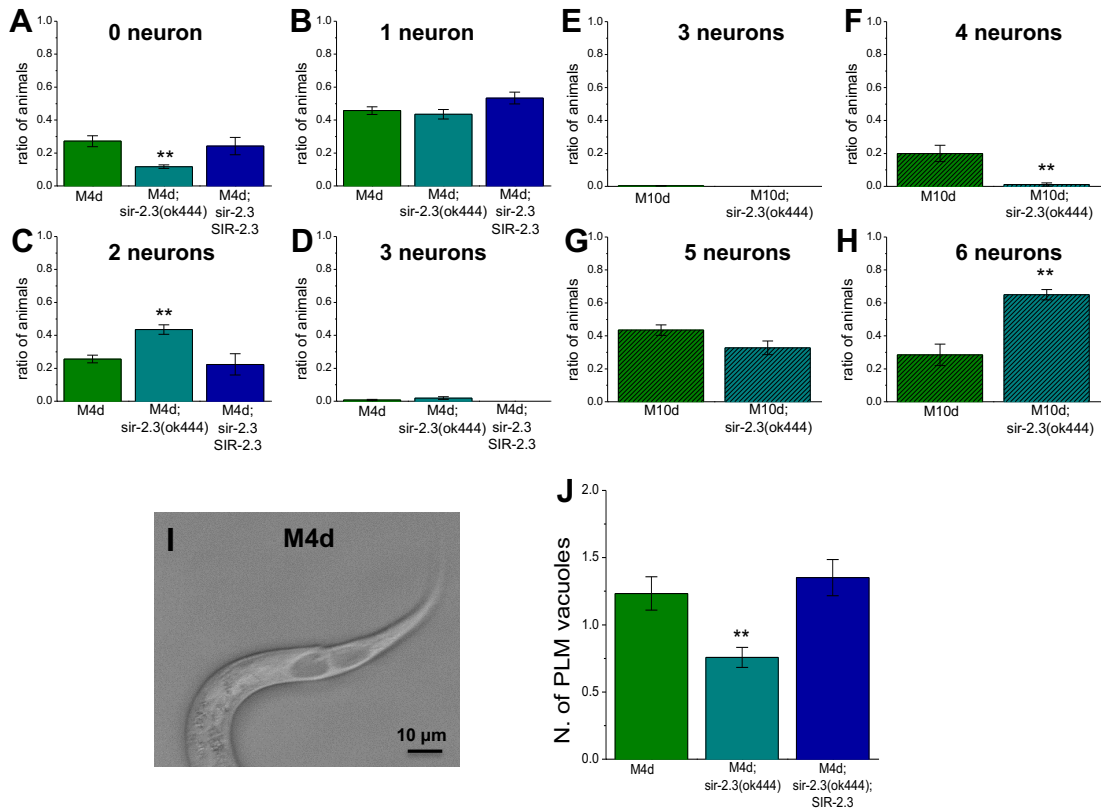


Fig. 4. Knock-out of mitochondrial *sir-2.3* protects against *mec-4(d)* and *mec-10(d)*-induced neuronal death. **A-D:** Quantification of the ratio of animals with 0, 1, 2 and 3 surviving touch neurons in *mec-4(d)*, *mec-4(d);sir-2.3* knock-out and *mec-4(d);sir-2.3;SIR-2.3* rescue strains. Number of experiments was 23, 23 and 4, with at least 50 animals per strain analyzed in each experiment. P was 0.0002 and 0.0001 by ANOVA with Bonferroni correction. **E-H:** Ratio of *mec-10(d)* expressing animals with 3, 4, 5 and 6 surviving touch neurons. Number of experiments was 4 each, with at least 50 animals per strain analyzed in each experiment. P was 0.01 and 0.0024 by t-Test. **I:** Photograph of a tail of an L1 *mec-4(d)* mutant *C. elegans* showing a necrotic swollen PLM touch neuron, visible as a large vacuole. Scale bar is 10 μ m. **J:** Quantification of the number of swollen PLMs in L1 *mec-4(d)*, *mec-4(d);sir-2.3* knock-out and *mec-4(d);sir-2.3;SIR-2.3* rescue strains. Number of experiments was 5, 5 and 4, with at least 50 animals per strain analyzed in each experiment. Data are expressed as mean \pm SE. P was 0.014 by ANOVA with Bonferroni correction.

Mec-4(d) begins to cause toxicity in touch neurons as soon as it becomes expressed early in development and at the first larval stage L1 touch neurons already show the signs of necrotic cell death as they appear swollen and filled with fluid (Fig. 4 I) [49]. To establish whether knock-out of *sir-2.3* affords protection at these early developmental stages, we examined touch neurons in L1 larvae. We counted the number of PLM vacuoles in *mec-4(d)*, *mec-4(d);sir-2.3* and *mec-4(d);sir-2.3;SIR-2.3* rescue and found that there were fewer swollen PLM touch

neurons in *sir-2.3* knock-out animals (0.75 ± 0.07 versus 1.2 ± 0.12 in *mec-4(d)* and 1.35 ± 0.13 in *mec-4(d);sir-2.3;SIR-2.3*, respectively). These results support that the protective effects of knock-out of mitochondrial *sir-2.3* are present early on in development suggesting that the mechanisms involved are likely not grossly developmentally regulated. To rule out an effect of the knock-out of *sir-2.3* on *mec-4(d)* expression level in touch neurons, which would result in changes on the extent of neuronal death, we quantified fluorescence in touch neurons expressing GFP tagged MEC-4. We found that the knock-out of *sir-2.3* does not change the level of expression of MEC-4::GFP transgene (Fig.5). Taken together these results support that knock-out of *sir-2.3* provides protection against necrotic cell death induced by channel hyperactivation.

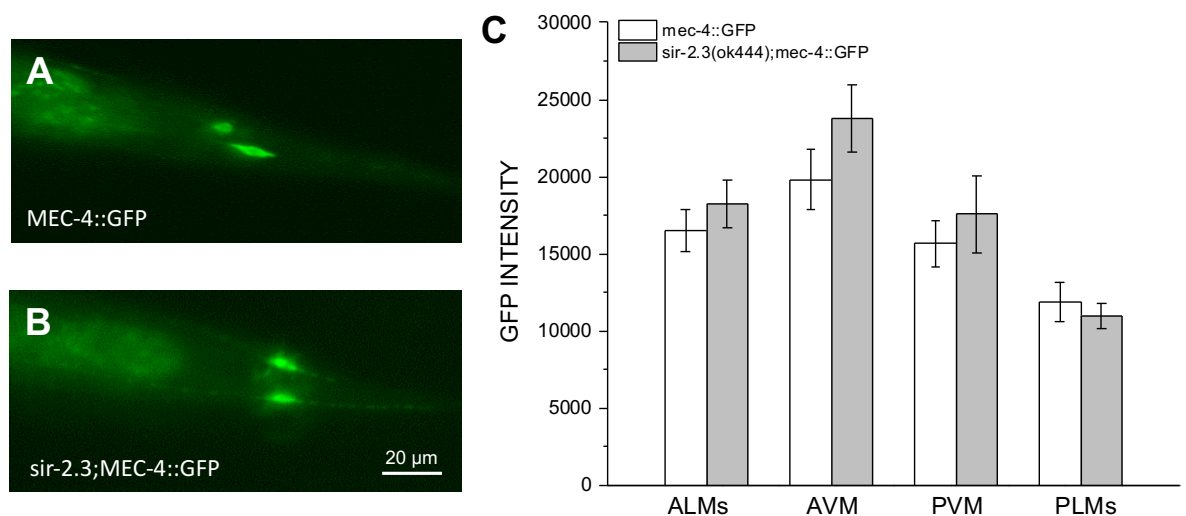


Fig. 5: Similar levels of expression of a MEC-4::GFP transgene in wild type and *sir-2.3* knock-out animals. A and B: Representative photographs of tails of transgenic wild type (A) and *sir-2.3(ok444)* (B) animals expressing MEC-4::GFP in PLM's touch neurons. Scale bar is 20 μ m. **C:** Quantification of MEC-4::GFP intensity in PLM's, PVM, ALM's and AVM touch neurons of N2 and *sir-2.3(ok444)* animals. N= 30 and 34 *p_{mec-4}mec-4::GFP* and *sir-2.3(ok444); p_{mec-4}mec-4::GFP* animals, respectively.

3.4 BLOCK OF THE NICOTINAMIDE ADENINE DINUCLEOTIDE (NAD) SALVAGE PATHWAY PROTECTS AGAINST NEURONAL DEATH

Sirtuins use NAD^+ as substrate in their de-acetylation reaction. NAD^+ is both synthesized de novo from tryptophan and by recycling of degraded NAD^+ products such as nicotinamide through the salvage pathway (Fig. 6 A) [129, 130]. A key enzyme of the NAD^+ salvage pathway in invertebrates is the nicotinamidase encoded by the PNC1 gene (*pnc-1* in *C. elegans*), which converts nicotinamide into nicotinic acid [131, 132]. Inhibition or knock-out of *pnc-1* reduces the level of NAD^+ and increases the concentration of nicotinamide in the cell, as this *pnc-1* substrate is no longer metabolized. The end result of both these effects is inhibition of sirtuins as nicotinamide functions in a negative feedback loop to inhibit sirtuins function [133].

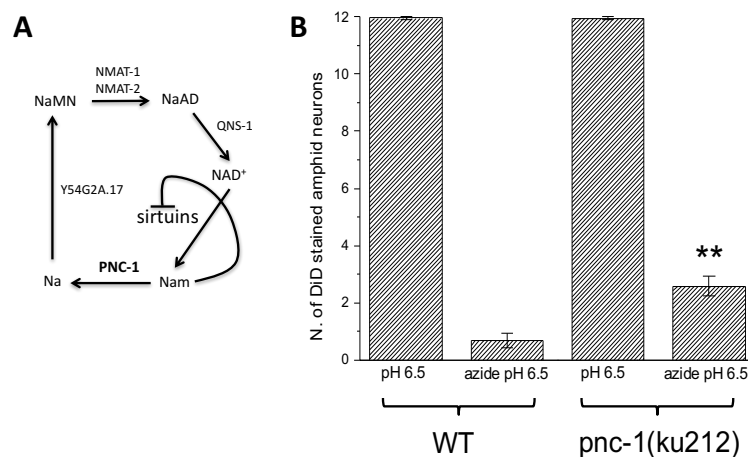


Fig. 6. Block of the NAD^+ salvage pathway by null mutation in *pnc-1* protects neurons from hypoxic ischemia. **A:** schematic representation of the invertebrate NAD^+ salvage pathway. In invertebrates PNC-1 converts nicotinamide into nicotinic acid. A null mutation in *pnc-1* leads to reduced availability of NAD^+ and accumulation of its substrate nicotinamide, which in turn inhibits the activity of sirtuins. **B:** Average number of DiD stained amphid sensory neurons in WT and *pnc-1(ku212)* mutant in control conditions (pH 6.5) and under conditions of chemical hypoxia (100 mM azide at pH 6.5). Data are expressed as mean \pm SE. Number of animals was 24 and 25 for wild type and 23 and 25 for *pnc-1(ku212)* in control conditions and azide respectively. P was 0.000029 by Student's t-test.

We thus reasoned that blocking the NAD⁺ salvage pathway may produce the same effect on neuronal death as the knock-out of sir-2.3. To test this hypothesis, we acquired the pnc-1(ku212) mutant, which encodes a premature stop mutation in both pnc-1a and pnc-1b isoforms leading to complete loss of enzymatic activity [134]. Pnc-1(ku212) mutants have developmental defects in the reproductive system, including delayed development of the gonad and necrosis of the four uterine cells, and they are egg-laying defective [134, 135]. Contrarily to what it may have been expected from the necrosis of the uterine cells in pnc-1(ku212) mutants, when we quantified the number of amphid sensory neurons that uptake DiD in pnc-1(ku212) animals treated with azide, we found that they were more than in wild type (2.58 +/- 0.34 versus 0.68 +/- 0.23, Fig. 6 B). We interpret these results to suggest that inhibition of the activity of sirtuins via reduced NAD⁺ and increased nicotinamide in pnc-1(ku212) is protective in cells under ischemic insult, which is consistent with data shown in Fig. 2 and 4.

3.5 BLOCK OF GLUCOSE METABOLISM REDUCES *mec-4(d)* INDUCED NEURONAL DEATH

We showed that the protective effect of diapause and knock-out of sir-2.3 are quantitatively similar. To learn more about the nature of the mechanisms underlying these protective effects, we first turned to the use of 2-Deoxy-D-glucose to control worm metabolism. 2-Deoxy-D-glucose (2-DG) is a glucose analogue that is taken up by the glucose transporters and is phosphorylated but that cannot be fully metabolized. Thus, 2-DG-6-phosphate accumulates in the cell and interferes with carbohydrate metabolism by inhibiting glycolytic enzymes. We tested the effect of 2-DG on *mec-4(d)*-induced neuronal death by culturing worms on plates containing 10 mM 2-DG. We found that that in *mec-4(d)* animals cultured

in these conditions, neuronal death is reduced. While the ratio of animals with 1 surviving touch neuron remained unchanged, the ratio of animals with 0 and 2 surviving touch neurons went from 0.31 +/- 0.04 and 0.21 +/- 0.03 for animals cultured on standard plates to 0.22 +/- 0.08 and 0.45 +/- 0.07 for animals cultured on 2-DG plates respectively (fig. 7 A-D). Importantly, surviving neurons appeared also healthier as they retained at least part of their neuronal processes (Fig. 7 E). Thus, block of glycolysis provides protection against *mec-4(d)*-induced neuronal death.

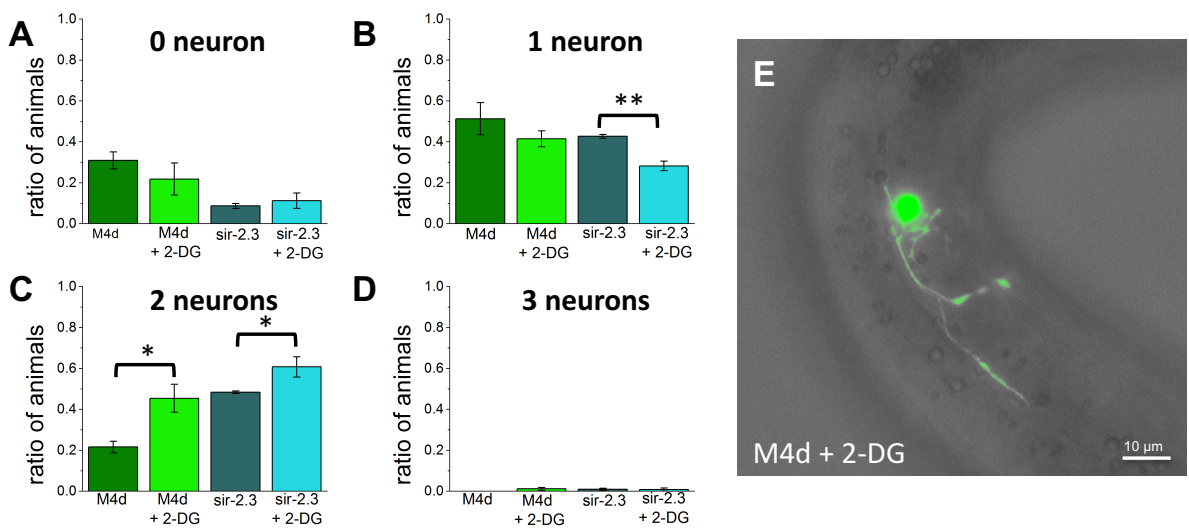


Fig. 7. Protection afforded by block of glycolysis in the presence and absence of SIR-2.3. A-D: Ratio of animals with 0, 1, 2 or 3 surviving touch neurons that were either grown on standard plates or on plates containing 5 mM 2-DG for 48 hours. Number of experiments was 4 each, with at least 30 animals in each experiment. Data are expressed as mean +/- SE. P was 0.0012, 0.018 and 0.048, by t-Test. E: Photograph of a ALM touch neuron in a *mec-4(d)* animals grown on 2-DG plate. The neuronal processes are still intact and show some arborization. Scale bar is 10 μm.

Calixto and colleagues showed that the protective effect of diapause and caloric restriction on *mec-4(d)*-induced touch neurons degeneration is mediated by the Insulin/IGF-1-like signaling pathway via activation of antioxidant mechanisms. Our results support that treatment with 2-DG mimics the protective effects of diapause. We also found that knock-out of mitochondrial sirtuin sir-2.3 mediates a similar

level of protection in *mec-4(d)*, *mec-10(d)* and azide mediated cell death. Thus, we next wondered whether the protection afforded by 2-DG treatment and knock-out of *sir-2.3* is mediated by the same mechanisms. To test this possibility, we treated *mec-4(d);sir-2.3* mutants with 2-DG and compared the extent of cell death with untreated animals and with *mec-4(d)* animals treated with 2-DG. We found that 2-DG enhances protection in *mec-4(d);sir-2.3* beyond the level seen in untreated animals and in *mec-4(d)* animals treated with 2-DG (ratio of animals with 0, 1 and 2 surviving touch neurons in *mec-4(d);sir-2.3* was 0.11 +/- 0.04, 0.28 +/- 0.02 and 0.60 +/- 0.05 respectively Fig. 7 A-D). These results support that 2-DG and knock-out of *sir-2.3* mediate protection through two different mechanisms.

3.6 EXPERIMENTS IN CELL CULTURE REVEAL A CELL AUTONOMOUS EFFECT OF 2-DG DEPENDENT ON KNOCK-OUT OF *sir-2.3*

The protection of touch neurons degeneration mediated by diapause entry in *mec-4(d)* animals is via the insulin/IGF-1-like signaling pathway involving the insulin receptor *daf-2* and therefore is non-cell autonomous. However, it is unclear whether protection mediated by *sir-2.3* knock-out is cell-autonomous or not. To test the dependence of protection afforded by knock-out of *sir-2.3* on other tissues/cells, we performed experiments in cell culture, where cell to cell contacts are rare and where substances released by other cells are significantly diluted in the culturing media.

C. elegans embryonic cells can be dissociated and cultured in vitro where they differentiate and express cell specific markers. We have previously shown that 24

hours after plating, *C. elegans* touch neurons are differentiated and morphologically resemble touch neurons in vivo, express GFP under the control of *mec-4* promoter and undergo cell death when they express *mec-4(d)*. We cultured *C. elegans* embryonic cells from wild type, *mec-4(d)* and *mec-4(d);sir-2.3(ok444)* both in control conditions and in the presence of 2-DG. Touch neurons were labeled by expression of GFP under the control of the *mec-4* promoter (Fig. 8 A-F). We thus quantified the ratio of touch neurons under the two culturing conditions for all three genetic backgrounds. As expected, we found that touch neurons make up ~5% of the embryonic cells, elongate one single neuronal process and express GFP under the control of the *mec-4* promoter. Treatment with 2-DG does not change wild type touch neurons ratio in the cell population or their morphology (Fig. 8 A, B and G). As previously published, we found that *mec-4(d)* touch neurons undergo degeneration in cell culture. The rarely surviving *mec-4(d)* touch neurons do not have neuronal processes or have short processes (Fig. 8 C and G). Importantly addition of 2-DG to *mec-4(d)* touch neurons does not rescue them from degeneration (Fig. 8 G). These data support the results from Calixto and colleagues showing that diapause and caloric restriction rescue *mec-4(d)* touch neurons from degeneration via the insulin/IGF-1-like signaling pathway, which is disrupted in culture.

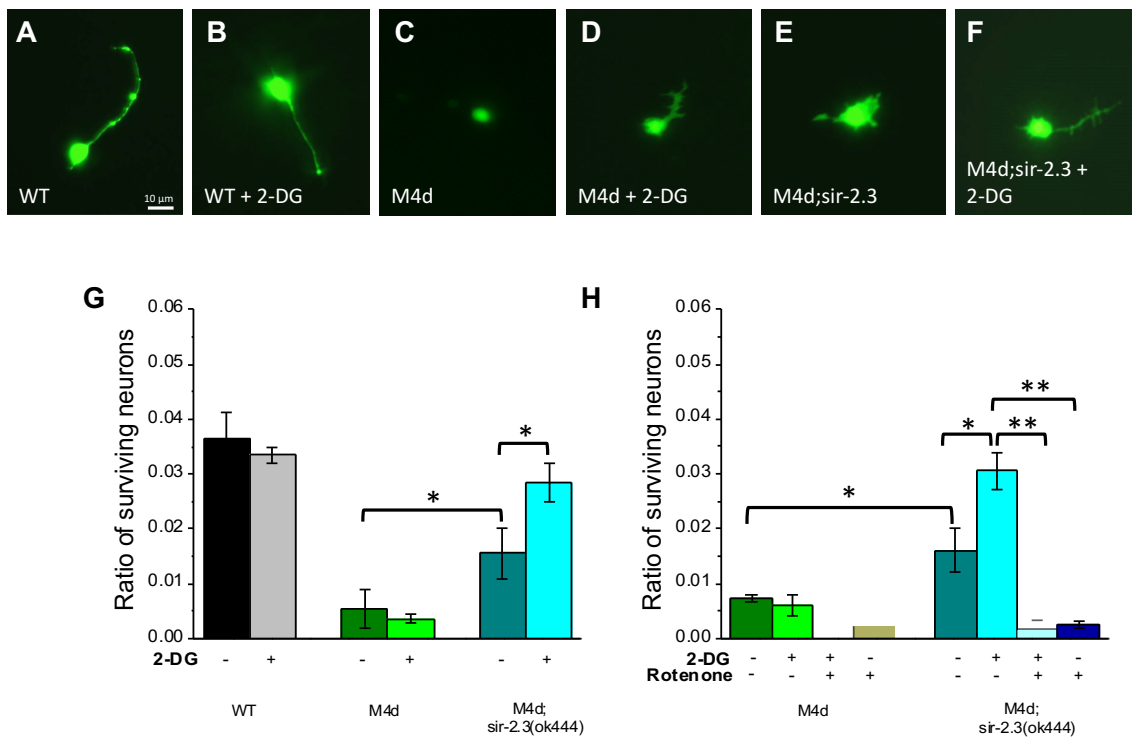


Fig 8. Effect of block of glycolysis and knock-out of *sir-2.3* on *mec-4(d)*-induced neuronal death in cultured cells. A-F: Fluorescent images of wild type, *mec-4(d)* and *sir-2.3;mec-4(d)* touch neurons expressing $P_{mec-4}::GFP$ cultured *in vitro*. Cells were in control media (A,C,E) or in media containing 10 mM 2-deoxy-glucose(2-DG)(B,D,F). Scale bar is 10 μ m. **G:** Quantification of surviving touch neurons in culture for the genetic strains shown in the micrographs, in control media and in media containing 10 mM 2-DG. Data are expressed as the means \pm SE. Same results were obtained in 5 independently performed experiments. N is 2 coverslips for each strain (wild type, *mec-4(d)* and *sir-2.3;mec-4(d)*) and for both conditions (control and 10 mM 2-DG respectively), with at least 10 fields scored per coverslip. **H:** Quantification of surviving touch neurons in culture for an experiment similar to the one shown in panel G for *mec-4(d)* and *sir-2.3;mec-4(d)*. In this case the culturing conditions were: control, 10 mM 2-DG, 2.5 μ M Rotenone and 10 mM 2-DG + 2.5 μ M Rotenone. N is 2 coverslips each with at least 10 fields scored per coverslip. P was 0.039 and 0.015 (panel G) and 0.019, 0.007, 0.00007 and 0.00006 (panel H) by ANOVA with Bonferroni correction.

Interestingly though and in line with the results of *in vivo* experiments (Fig. 7 A-D), knock-out of *sir-2.3* still protects neurons from neuronal death in culture and this protective effect is further enhanced by treatment with 2-DG. These results, support that the rescue of neuronal death afforded by *sir-2.3* knock-out is cell-autonomous, that it's mediated by a mechanism that at least in part differs from the insulin/IGF-1-like signaling pathway and that enables protection afforded by 2-DG in culture.

To test whether the protective effect of sir-2.3 knock-out and 2-DG could be overwritten by block of mitochondrial function, we incubated cells with rotenone, which blocks complex I in the mitochondrial respiratory chain. Under these conditions, we found that the protective effect of sir-2.3 knock-out and of 2-DG in this mutant was completely lost, suggesting the requirement of mitochondrial function for protection to be carried out (Fig. 7 H).

3.7 MITOHORMETIC ELEVATION OF ROS AND PROTECTION AGAINST NEURONAL DEGENERATION

In *mec-4(d)* expressing touch neurons undergoing degeneration Reactive Oxygen Species (ROS) are elevated and treatment with antioxidants provides protection. Given, the striking similarities between *mec-4(d)* and azide-induced neuronal death, we hypothesized that ROS might be elevated also in animals treated with azide. To test this possibility, we stained wild type worms treated with 100 mM azide for 2 hours with the fluorescent dye DCF, which detects H₂O₂. As expected, we found that DCF fluorescence indicative of ROS was elevated (Fig. 9 A).

conditions, we found that ROS was 6 times more elevated in starved animals and animals treated with 2-DG as compared to animals cultured in the presence of food. These data suggest that mitohormesis is indeed operative in these conditions leading to protection against neuronal death, which we observe in starved animals or animals cultured in the presence of 2-DG treated with azide or expressing *mec-4(d)* (Fig. 2 G and 8 A-D). Interestingly, starvation only without treatment with azide, does not induce increase of ROS in wild type animals (Fig. 9 A).

When we compared levels of ROS in *sir-2.3(ok444)* mutants we noticed similarities and some key differences as compared to wild type. Similar to wild type, in *sir-2.3* animals ROS becomes elevated after 2 hours of azide treatment to a level that is similar to the one found in wild type animals (Fig. 9 A). These data suggest that protection afforded by knock-out of *sir-2.3* is not mediated by mitohormetic elevation of ROS, at least not in the presence of food. However, in dietary deprived animals and animals cultured in the presence of 2-DG and treated with azide, ROS increases only between 2 and 4 folds. Moreover, in the absence of azide, dietary deprivation per se induces ROS elevation in *sir-2.3* knock-out animals (fig.9 A and E). We interpret these results to suggest that knock-out of this sirtuin increases the animals sensitivity to dietary deprivation, which results in more robust and rapid protection.

4. DISCUSSION

In this work, we investigated the role of *C. elegans* mitochondrial sirtuin SIR-2.3, homologous to mammalian SIRT4, in two distinct models of neuronal death with morphological and molecular features of necrosis akin necrosis that occurs in cerebral ischemia. We showed that knock-out of *sir-2.3* is protective against neuronal death in both models, both under severe and mild toxic insults, and that protection is enhanced by dietary deprivation and block of glycolysis. We further showed that this mechanism of protection is cell autonomous and does not require interaction with other cells or secreted molecules. Protection afforded by *sir-2.3* knock-out is distinct from that afforded by entry into diapause and may share only downstream targets. Indeed, we showed that in ischemic conditions dietary deprivation induce mitohormetic elevation of ROS both in wild type and *sir-2.3* knock-out animals, however the timing, conditions under which this occurs and the extent vary. We conclude that knock-out of mitochondrial sirtuin *sir-2.3* results in changes of mitochondrial function, that result in more efficient response to toxic insults, suggesting a deleterious role of SIRT4 during the ischemic processes that must to be further investigated.

4.1 INSIGHTS INTO THE ROLE OF MITOHORMETIC ROS IN NEURONAL PROTECTION MEDIATED BY HYPERACTIVE CHANNELS IN ISCHEMIA

Elevation of ROS is a mechanism of cellular toxicity operative in many disease states including neurodegenerative conditions and cancer. In *mec-4(d)*-induced neuronal death calcium enters the cell through the hyperactivated MEC-4(d) channel, leading to calcium release from the endoplasmic reticulum, mitochondrial

dysfunction and ROS generation. Calixto and colleagues showed that during diapause or under caloric restriction inhibition of the insulin pathway leads to *daf-16*-mediated activation of antioxidant mechanisms including SODs and catalases, which ultimately lead to protection from neuronal death. However, it was not clear whether *daf-16* directly mediates the transcription of anti-oxidant genes. We showed that ROS becomes markedly elevated under dietary deprivation and following treatment with 2-DG early on during the toxic insult in a model of chemical ischemia (Fig 9). The increase of ROS under dietary deprivation and in 2-DG is much higher than in animals cultured ad libitum, yet protection is observed under these conditions. We interpret these results to suggest that such marked increase of ROS functions as mitohormetic signal to induce activation of anti-oxidant mechanisms. A mitohormetic effect of ROS has been previously suggested to explain the effect of caloric restriction in other models. Interestingly, the protective effect of 2-DG is not present in culture (Fig. 8), suggesting that under these experimental conditions mitohormetic increase of ROS is not occurring or is strongly attenuated and/or downstream activation of anti-oxidant mechanisms is absent in culture. We suggest that this is because FBS used in the culture media contains insulin like ligands which likely interact with DAF-2 to maintain the insulin pathway active which results in suppression of DAF-16 translocation into the nucleus.

4.2 KNOCK-OUT OF MITOCHONDRIAL SIRTUIN *sir-2.3* AND ROS

Our data suggest that when *sir-2.3* is knocked-out, an additional mechanism of protection is activated. SIR-2.3 shares the highest homology with mammalian SIRT4 (42% identity and 62% similarity). Like SIRT4, SIR-2.3 is expressed in neurons and is localized in mitochondria [136]. The enzymatic activity of SIRT4

has been a subject of debate because a SIRT4-mediated deacetylase activity could not be initially identified. However, recently SIRT4 has been reported to have specific deacetylase activity toward malonyl CoA decarboxylase. Similarly, sir-2.3 mediated deacetylase activity has not been demonstrated, however, sir-2.3 interacts with several highly acetylated mitochondrial carboxylases including mitochondrial biotin-dependent carboxylases, pyruvate carboxylase, propionyl-CoA carboxylase and methylcrotonyl-CoA carboxylase, suggesting that indeed sir-2.3 controls their level of acetylation. SIRT4 possesses also ADP-ribosylase activity and one of its targets is the mitochondrial enzyme glutamate dehydrogenase (GDH) [136], which mediates the conversion of glutamate into alpha-keto glutarate, a Krebs cycle intermediate. By mediating ADP-ribosylation of GDH, SIRT4 inhibits the activity of this enzyme resulting in repression of glutamine metabolism. Knock-out of SIRT4 is expected to induce increase of the concentration of alpha-ketoglutarate due to disinhibition of GDH. Interestingly, alpha-ketoglutarate is a ROS scavenger. Thus, knock-out of SIRT4 may predispose the cell to increased resistance to oxidative stress especially when paired with block of glycolysis, which forces the cell to use amino acid metabolism for energy production. Moreover, compared to other sirtuins, SIRT4 has a peculiar expression in brain and is involved in controlling serotonergic pathway, which is pivotal in regulating oxidative stress, and insulin/IGF-1 signaling pathway in neurons [137].

We do not know whether SIR-2.3 has ADP-ribosylase activity, however, it is interesting to note that a transgenic strain carrying a GFP tagged sir-2.3 transgene shows severe loss of resistance to oxidative stress (paraquat). Our data do not show more extensive neuronal death in transgenic worms overexpressing *sir-2.3*

(Fig 2), but they show that ROS production is strongly attenuated in *sir-2.3* knock-out animals under conditions of chemical ischemia, when paired with dietary deprivation or block of glycolysis (2-DG) (Fig. 9). An implication of the amino-acid metabolism and of ROS scavenger alpha-ketoglutarate in the protection against neuronal death mediated by knock-out of *sir-2.3* is further supported by our results in cell culture. Here, the effect of 2-DG on neuronal survival is even more robust than in vivo (compare Fig. 7 with Fig. 8). We suggest that this is due to the culturing conditions. Indeed, the culture media used for the treatment with 2-DG contains glutamine, which is expected to further increase the activity of GDH in the absence of *sir-2.3*. Interestingly, *sir-2.3* knock-out animals show elevated ROS under dietary deprivation in the absence of toxic insult (Fig. 8). This result is again consistent with elevated levels of alpha-ketoglutarate in *sir-2.3* knock-out strain under conditions that force the cell to switch to amino-acid metabolism, which stimulates the Krebs cycle and therefore induce elevation of ROS via both the Krebs cycle and the respiratory chain. As a further support that mitohormetic production of ROS mediates the protective effects of knock-out of *sir-2.3* and caloric restriction, block of the complex I of the respiratory chain by rotenone, completely eliminates protection (Fig. 8). Indeed, under these conditions, it is expected that the majority of ROS production is eliminated. In line with our observations, it has been recently shown that direct activation of GDH by activators protects against brain ischemia and reperfusion.

Importantly, our data show that protection afforded by block of glycolysis has distinct effects depending on whether *sir-2.3* is present or not in the cell. When *sir-2.3* is present the effect is mainly mediated by the insulin pathway, as Calixto and colleagues have shown. When *sir-2.3* is knocked-out, the effect does not

require interaction with other cells or secreted molecules. We interpret this result as supportive evidence that 2-DG or dietary restriction/deprivation force the cell to switch to amino acid metabolism and therefore production of ROS scavenger alpha-ketoglutarate and this is how protection is mediated under these conditions. Interestingly, when the sir-2.3 knock-out animals are cultured at libitum and are subjected to chemical ischemia, they show an increase in ROS early on during treatment that is identical to the increase in ROS observed in wild type animals (Fig. 8, first 4 bars). This result suggests that the protection mediated by knock-out of sir-2.3 per se is independent of ROS and may be related to sir-2.3 deacetylase activity.

We have shown here that the knock-out of mitochondrial sirtuin protects neurons from ischemic damage, especially when paired with dietary deprivation or block of glycolysis, which forces the cell to switch to amino acid catabolism through activation of glutamate dehydrogenase. Furthermore, we showed that protection appears to be mediated by mitohormetic elevation of ROS. Our work extends our understanding of mitochondrial sirtuins and of the interplay of glycolysis, Krebs cycle and respiratory chain in the control of the cellular redox state and survival. Given, the parallelism between the models of neuronal death used in this work and ischemia in humans, our work suggests novel approaches targeting SIRT4 and cautions about the use of non-specific sirtuins activators or inhibitors.

5. BIBLIOGRAPHY

1. Gibb, W.R. and A.J. Lees, *The relevance of the Lewy body to the pathogenesis of idiopathic Parkinson's disease*. J Neurol Neurosurg Psychiatry, 1988. **51**(6): p. 745-52.
2. Wong, Y.C. and D. Krainc, *alpha-synuclein toxicity in neurodegeneration: mechanism and therapeutic strategies*. Nat Med, 2017. **23**(2): p. 1-13.
3. Savica, R., B.F. Boeve, and G. Logroscino, *Epidemiology of alpha-synucleinopathies: from Parkinson disease to dementia with Lewy bodies*. Handb Clin Neurol, 2016. **138**: p. 153-8.
4. Jenner, P., *Oxidative stress in Parkinson's disease*. Ann Neurol, 2003. **53 Suppl 3**: p. S26-36; discussion S36-8.
5. Qiu, C., et al., *Association of blood pressure and hypertension with the risk of Parkinson disease: the National FINRISK Study*. Hypertension, 2011. **57**(6): p. 1094-100.
6. de Rijk, M.C., et al., *Prevalence of parkinsonism and Parkinson's disease in Europe: the EUROPARKINSON Collaborative Study. European Community Concerted Action on the Epidemiology of Parkinson's disease*. J Neurol Neurosurg Psychiatry, 1997. **62**(1): p. 10-5.
7. Delamarre, A. and W.G. Meissner, *Epidemiology, environmental risk factors and genetics of Parkinson's disease*. Presse Med, 2017.
8. Kitada, T., et al., *Mutations in the parkin gene cause autosomal recessive juvenile parkinsonism*. Nature, 1998. **392**(6676): p. 605-8.
9. Trachootham, D., et al., *Redox regulation of cell survival*. Antioxid Redox Signal, 2008. **10**(8): p. 1343-74.
10. Johnson, W.M., A.L. Wilson-Delfosse, and J.J. Mielay, *Dysregulation of glutathione homeostasis in neurodegenerative diseases*. Nutrients, 2012. **4**(10): p. 1399-440.
11. Etminan, M., B.C. Carleton, and A. Samii, *Non-steroidal anti-inflammatory drug use and the risk of Parkinson disease: a retrospective cohort study*. J Clin Neurosci, 2008. **15**(5): p. 576-7.
12. Pallone, J.A., *Introduction to Parkinson's disease*. Dis Mon, 2007. **53**(4): p. 195-9.
13. Weintraub, D., C.L. Comella, and S. Horn, *Parkinson's disease--Part 1: Pathophysiology, symptoms, burden, diagnosis, and assessment*. Am J Manag Care, 2008. **14**(2 Suppl): p. S40-8.
14. Zesiewicz, T.A., et al., *Practice Parameter: treatment of nonmotor symptoms of Parkinson disease: report of the Quality Standards Subcommittee of the American Academy of Neurology*. Neurology, 2010. **74**(11): p. 924-31.
15. Morgan, J.P. and J.R. Bianchine, *The clinical pharmacology of levodopa*. Ration Drug Ther, 1971. **5**(1): p. 1-8.
16. Lewitt, P.A., *Levodopa for the treatment of Parkinson's disease*. N Engl J Med, 2008. **359**(23): p. 2468-76.
17. Schrag, A. and N. Quinn, *Dyskinesias and motor fluctuations in Parkinson's disease. A community-based study*. Brain, 2000. **123 (Pt 11)**: p. 2297-305.
18. Chase, T.N. and J.D. Oh, *Striatal dopamine- and glutamate-mediated dysregulation in experimental parkinsonism*. Trends Neurosci, 2000. **23**(10 Suppl): p. S86-91.

19. Smith, T.S., W.D. Parker, Jr., and J.P. Bennett, Jr., *L-dopa increases nigral production of hydroxyl radicals in vivo: potential L-dopa toxicity?* Neuroreport, 1994. **5**(8): p. 1009-11.
20. Obeso, J.A., C.W. Olanow, and J.G. Nutt, *Levodopa motor complications in Parkinson's disease*. Trends Neurosci, 2000. **23**(10 Suppl): p. S2-7.
21. Ramassamy, C., *Emerging role of polyphenolic compounds in the treatment of neurodegenerative diseases: a review of their intracellular targets*. Eur J Pharmacol, 2006. **545**(1): p. 51-64.
22. Holst, B. and G. Williamson, *A critical review of the bioavailability of glucosinolates and related compounds*. Nat Prod Rep, 2004. **21**(3): p. 425-47.
23. Noyan-Ashraf, M.H., Z. Sadeghinejad, and B.H. Juurlink, *Dietary approach to decrease aging-related CNS inflammation*. Nutr Neurosci, 2005. **8**(2): p. 101-10.
24. Kraft, A.D., D.A. Johnson, and J.A. Johnson, *Nuclear factor E2-related factor 2-dependent antioxidant response element activation by tert-butylhydroquinone and sulforaphane occurring preferentially in astrocytes conditions neurons against oxidative insult*. J Neurosci, 2004. **24**(5): p. 1101-12.
25. Weber, C.A. and M.E. Ernst, *Antioxidants, supplements, and Parkinson's disease*. Ann Pharmacother, 2006. **40**(5): p. 935-8.
26. Moskowitz, M.A., E.H. Lo, and C. Iadecola, *The science of stroke: mechanisms in search of treatments*. Neuron, 2010. **67**(2): p. 181-98.
27. Redon, J., et al., *Stroke mortality and trends from 1990 to 2006 in 39 countries from Europe and Central Asia: implications for control of high blood pressure*. Eur Heart J, 2011. **32**(11): p. 1424-31.
28. Saposnik, G., et al., *IScore: a risk score to predict death early after hospitalization for an acute ischemic stroke*. Circulation, 2011. **123**(7): p. 739-49.
29. Bushnell, C., et al., *Guidelines for the prevention of stroke in women: a statement for healthcare professionals from the American Heart Association/American Stroke Association*. Stroke, 2014. **45**(5): p. 1545-88.
30. Mehta, R.H., et al., *Race/Ethnic differences in the risk of hemorrhagic complications among patients with ischemic stroke receiving thrombolytic therapy*. Stroke, 2014. **45**(8): p. 2263-9.
31. Baron, J.C., *[The pathophysiology of acute cerebral ischemia: clinical approach using physiologic imaging]*. Rev Neurol (Paris), 1999. **155**(9): p. 639-43.
32. Sohrabji, F., M.J. Park, and A.H. Mahnke, *Sex differences in stroke therapies*. J Neurosci Res, 2017. **95**(1-2): p. 681-691.
33. Hagberg, H., et al., *Ischemia-induced shift of inhibitory and excitatory amino acids from intra- to extracellular compartments*. J Cereb Blood Flow Metab, 1985. **5**(3): p. 413-9.
34. Lai, T.W., S. Zhang, and Y.T. Wang, *Excitotoxicity and stroke: identifying novel targets for neuroprotection*. Prog Neurobiol, 2014. **115**: p. 157-88.
35. Aarts, M.M., M. Arundine, and M. Tymianski, *Novel concepts in excitotoxic neurodegeneration after stroke*. Expert Rev Mol Med, 2003. **5**(30): p. 1-22.
36. Hinshaw, M., et al., *Metastatic transitional cell carcinoma of the bladder presenting as genital edema*. J Am Acad Dermatol, 2004. **51**(1): p. 143-5.
37. Bano, D. and P. Nicotera, *Ca²⁺ signals and neuronal death in brain ischemia*. Stroke, 2007. **38**(2 Suppl): p. 674-6.
38. Denes, A., et al., *Experimental stroke-induced changes in the bone marrow reveal complex regulation of leukocyte responses*. J Cereb Blood Flow Metab, 2011. **31**(4): p. 1036-50.
39. Jin, R., G. Yang, and G. Li, *Inflammatory mechanisms in ischemic stroke: role of inflammatory cells*. J Leukoc Biol, 2010. **87**(5): p. 779-89.

40. Hong, L.Z., X.Y. Zhao, and H.L. Zhang, *p53-mediated neuronal cell death in ischemic brain injury*. *Neurosci Bull*, 2010. **26**(3): p. 232-40.
41. Radi, E., et al., *Apoptosis and oxidative stress in neurodegenerative diseases*. *J Alzheimers Dis*, 2014. **42 Suppl 3**: p. S125-52.
42. Nitatori, T., et al., *Delayed neuronal death in the CA1 pyramidal cell layer of the gerbil hippocampus following transient ischemia is apoptosis*. *J Neurosci*, 1995. **15**(2): p. 1001-11.
43. Price, M.P., et al., *The DRASIC cation channel contributes to the detection of cutaneous touch and acid stimuli in mice*. *Neuron*, 2001. **32**(6): p. 1071-83.
44. Askwith, C.C., et al., *DEG/ENaC ion channels involved in sensory transduction are modulated by cold temperature*. *Proc Natl Acad Sci U S A*, 2001. **98**(11): p. 6459-63.
45. Tavernarakis, N. and M. Driscoll, *Molecular modeling of mechanotransduction in the nematode *Caenorhabditis elegans**. *Annu Rev Physiol*, 1997. **59**: p. 659-89.
46. Drummond, H.A., F.M. Abboud, and M.J. Welsh, *Localization of beta and gamma subunits of ENaC in sensory nerve endings in the rat foot pad*. *Brain Res*, 2000. **884**(1--2): p. 1-12.
47. Chen, M., et al., *Direct interaction of YidC with the Sec-independent Pf3 coat protein during its membrane protein insertion*. *J Biol Chem*, 2002. **277**(10): p. 7670-5.
48. Jasti, J., et al., *Structure of acid-sensing ion channel 1 at 1.9 Å resolution and low pH*. *Nature*, 2007. **449**(7160): p. 316-23.
49. Driscoll, M. and M. Chalfie, *The mec-4 gene is a member of a family of *Caenorhabditis elegans* genes that can mutate to induce neuronal degeneration*. *Nature*, 1991. **349**(6310): p. 588-93.
50. Bianchi, L. and M. Driscoll, *Heterologous expression of *C. elegans* ion channels in *Xenopus* oocytes*. *WormBook*, 2006: p. 1-16.
51. Canessa, C.M., A.M. Merillat, and B.C. Rossier, *Membrane topology of the epithelial sodium channel in intact cells*. *Am J Physiol*, 1994. **267**(6 Pt 1): p. C1682-90.
52. Chalfie, M. and E. Wolinsky, *The identification and suppression of inherited neurodegeneration in *Caenorhabditis elegans**. *Nature*, 1990. **345**(6274): p. 410-6.
53. Xiong, Z.G., et al., *Neuroprotection in ischemia: blocking calcium-permeable acid-sensing ion channels*. *Cell*, 2004. **118**(6): p. 687-98.
54. Xu, K., N. Tavernarakis, and M. Driscoll, *Necrotic cell death in *C. elegans* requires the function of calreticulin and regulators of Ca(2+) release from the endoplasmic reticulum*. *Neuron*, 2001. **31**(6): p. 957-71.
55. Bernaudin, F. and S. Verlhac, *[Stroke prevention in sickle-cell disease: results, hurdles and future perspectives]*. *Bull Acad Natl Med*, 2008. **192**(7): p. 1383-93; discussion 1393-4.
56. Cavallini, S., et al., *Effects of chemical ischemia in cerebral cortex slices. Focus on nitric oxide*. *Neurochem Int*, 2005. **47**(7): p. 482-90.
57. Bennett, M.V. and A. Pereda, *Pyramid power: principal cells of the hippocampus unite!* *Brain Cell Biol*, 2006. **35**(1): p. 5-11.
58. Scott, B.A., M.S. Avidan, and C.M. Crowder, *Regulation of hypoxic death in *C. elegans* by the insulin/IGF receptor homolog DAF-2*. *Science*, 2002. **296**(5577): p. 2388-91.
59. Frye, R.A., *Phylogenetic classification of prokaryotic and eukaryotic Sir2-like proteins*. *Biochem Biophys Res Commun*, 2000. **273**(2): p. 793-8.

60. Imai, S., et al., *Transcriptional silencing and longevity protein Sir2 is an NAD-dependent histone deacetylase*. Nature, 2000. **403**(6771): p. 795-800.
61. Tsukamoto, Y., J. Kato, and H. Ikeda, *Silencing factors participate in DNA repair and recombination in Saccharomyces cerevisiae*. Nature, 1997. **388**(6645): p. 900-3.
62. Qin, W., et al., *Neuronal SIRT1 activation as a novel mechanism underlying the prevention of Alzheimer disease amyloid neuropathology by calorie restriction*. J Biol Chem, 2006. **281**(31): p. 21745-54.
63. Houtkooper, R.H., E. Pirinen, and J. Auwerx, *Sirtuins as regulators of metabolism and healthspan*. Nat Rev Mol Cell Biol, 2012. **13**(4): p. 225-38.
64. Chen, D., et al., *Increase in activity during calorie restriction requires Sirt1*. Science, 2005. **310**(5754): p. 1641.
65. Finkel, T., C.X. Deng, and R. Mostoslavsky, *Recent progress in the biology and physiology of sirtuins*. Nature, 2009. **460**(7255): p. 587-91.
66. Covington, J.D. and S. Bajpeyi, *The sirtuins: Markers of metabolic health*. Mol Nutr Food Res, 2016. **60**(1): p. 79-91.
67. Vaquero, A., et al., *Human SirT1 interacts with histone H1 and promotes formation of facultative heterochromatin*. Mol Cell, 2004. **16**(1): p. 93-105.
68. Bouras, T., et al., *SIRT1 deacetylation and repression of p300 involves lysine residues 1020/1024 within the cell cycle regulatory domain 1*. J Biol Chem, 2005. **280**(11): p. 10264-76.
69. Satoh, A., et al., *Sirt1 extends life span and delays aging in mice through the regulation of Nk2 homeobox 1 in the DMH and LH*. Cell Metab, 2013. **18**(3): p. 416-30.
70. Alcain, F.J. and J.M. Villalba, *Sirtuin activators*. Expert Opin Ther Pat, 2009. **19**(4): p. 403-14.
71. Outeiro, T.F., et al., *Sirtuin 2 inhibitors rescue alpha-synuclein-mediated toxicity in models of Parkinson's disease*. Science, 2007. **317**(5837): p. 516-9.
72. Vergnes, B., et al., *Targeted disruption of cytosolic SIR2 deacetylase discloses its essential role in Leishmania survival and proliferation*. Gene, 2005. **363**: p. 85-96.
73. Pagans, S., et al., *SIRT1 regulates HIV transcription via Tat deacetylation*. PLoS Biol, 2005. **3**(2): p. e41.
74. Tissenbaum, H.A. and L. Guarente, *Increased dosage of a sir-2 gene extends lifespan in Caenorhabditis elegans*. Nature, 2001. **410**(6825): p. 227-30.
75. Moroz, N., et al., *Dietary restriction involves NAD(+) -dependent mechanisms and a shift toward oxidative metabolism*. Aging Cell, 2014. **13**(6): p. 1075-85.
76. Hofer, A., et al., *Defining the action spectrum of potential PGC-1alpha activators on a mitochondrial and cellular level in vivo*. Hum Mol Genet, 2014. **23**(9): p. 2400-15.
77. Gomes, P.S., C. Matsuura, and Y.N. Bhambhani, *Effects of hypoxia on cerebral and muscle haemodynamics during knee extensions in healthy subjects*. Eur J Appl Physiol, 2013. **113**(1): p. 13-23.
78. Mostoslavsky, R., et al., *Genomic instability and aging-like phenotype in the absence of mammalian SIRT6*. Cell, 2006. **124**(2): p. 315-29.
79. Yang, B., et al., *The sirtuin SIRT6 deacetylates H3 K56Ac in vivo to promote genomic stability*. Cell Cycle, 2009. **8**(16): p. 2662-3.
80. Vakhrusheva, O., et al., *Sirt7 increases stress resistance of cardiomyocytes and prevents apoptosis and inflammatory cardiomyopathy in mice*. Circ Res, 2008. **102**(6): p. 703-10.

81. Borra, M.T., et al., *Conserved enzymatic production and biological effect of O-acetyl-ADP-ribose by silent information regulator 2-like NAD⁺-dependent deacetylases*. J Biol Chem, 2002. **277**(15): p. 12632-41.
82. Inoue, T., et al., *SIRT2, a tubulin deacetylase, acts to block the entry to chromosome condensation in response to mitotic stress*. Oncogene, 2007. **26**(7): p. 945-57.
83. Lombard, D.B., et al., *Mammalian Sir2 homolog SIRT3 regulates global mitochondrial lysine acetylation*. Mol Cell Biol, 2007. **27**(24): p. 8807-14.
84. Ahuja, N., et al., *Regulation of insulin secretion by SIRT4, a mitochondrial ADP-ribosyltransferase*. J Biol Chem, 2007. **282**(46): p. 33583-92.
85. Wirth, M., et al., *Mitochondrial SIRT4-type proteins in Caenorhabditis elegans and mammals interact with pyruvate carboxylase and other acetylated biotin-dependent carboxylases*. Mitochondrion, 2013. **13**(6): p. 705-20.
86. Song, R., et al., *The expression of Sirtuins 1 and 4 in peripheral blood leukocytes from patients with type 2 diabetes*. Eur J Histochem, 2011. **55**(1): p. e10.
87. Jeong, S.M., et al., *SIRT4 has tumor-suppressive activity and regulates the cellular metabolic response to DNA damage by inhibiting mitochondrial glutamine metabolism*. Cancer Cell, 2013. **23**(4): p. 450-63.
88. North, B.J., et al., *Preparation of enzymatically active recombinant class III protein deacetylases*. Methods, 2005. **36**(4): p. 338-45.
89. Haussinger, D., *Nitrogen metabolism in liver: structural and functional organization and physiological relevance*. Biochem J, 1990. **267**(2): p. 281-90.
90. Asthana, J., B.N. Mishra, and R. Pandey, *Acacetin promotes healthy aging by altering stress response in Caenorhabditis elegans*. Free Radic Res, 2016. **50**(8): p. 861-74.
91. Abete, P., et al., *Joint effect of physical activity and body mass index on mortality for acute myocardial infarction in the elderly: role of preinfarction angina as equivalent of ischemic preconditioning*. Eur J Cardiovasc Prev Rehabil, 2009. **16**(1): p. 73-9.
92. Raval, A.P., K.R. Dave, and M.A. Perez-Pinzon, *Resveratrol mimics ischemic preconditioning in the brain*. J Cereb Blood Flow Metab, 2006. **26**(9): p. 1141-7.
93. Pallos, J., et al., *Inhibition of specific HDACs and sirtuins suppresses pathogenesis in a Drosophila model of Huntington's disease*. Hum Mol Genet, 2008. **17**(23): p. 3767-75.
94. Almeida, R.P., et al., *Effect of Cognitive Reserve on Age-Related Changes in Cerebrospinal Fluid Biomarkers of Alzheimer Disease*. JAMA Neurol, 2015. **72**(6): p. 699-706.
95. Zhang, N., et al., *Control of the composition of Pt-Ni electrocatalysts in surfactant-free synthesis using neat N-formylpiperidine*. Nanoscale, 2016. **8**(5): p. 2548-53.
96. Della-Morte, D., et al., *Resveratrol pretreatment protects rat brain from cerebral ischemic damage via a sirtuin 1-uncoupling protein 2 pathway*. Neuroscience, 2009. **159**(3): p. 993-1002.
97. Wirth, M., et al., *Mitochondrial SIRT4-type proteins in Caenorhabditis elegans and mammals interact with pyruvate carboxylase and other acetylated biotin-dependent carboxylases*. Mitochondrion, 2013.
98. Viswanathan, M. and H.A. Tissenbaum, *C. elegans sirtuins*. Methods Mol Biol, 2013. **1077**: p. 39-56.
99. Fontana, L., S. Klein, and J.O. Holloszy, *Effects of long-term calorie restriction and endurance exercise on glucose tolerance, insulin action, and adipokine production*. Age (Dordr), 2010. **32**(1): p. 97-108.

100. Hulbert, A.J., et al., *Metabolic rate is not reduced by dietary-restriction or by lowered insulin/IGF-1 signalling and is not correlated with individual lifespan in Drosophila melanogaster*. *Exp Gerontol*, 2004. **39**(8): p. 1137-43.
101. Hand, S.C., et al., *Mechanisms of animal diapause: recent developments from nematodes, crustaceans, insects, and fish*. *Am J Physiol Regul Integr Comp Physiol*, 2016. **310**(11): p. R1193-211.
102. Calixto, A., J.S. Jara, and F.A. Court, *Diapause formation and downregulation of insulin-like signaling via DAF-16/FOXO delays axonal degeneration and neuronal loss*. *PLoS Genet*, 2012. **8**(12): p. e1003141.
103. Lee, J., et al., *2-Deoxy-D-glucose protects hippocampal neurons against excitotoxic and oxidative injury: evidence for the involvement of stress proteins*. *J Neurosci Res*, 1999. **57**(1): p. 48-61.
104. Schulz, T.J., et al., *Glucose restriction extends Caenorhabditis elegans life span by inducing mitochondrial respiration and increasing oxidative stress*. *Cell Metab*, 2007. **6**(4): p. 280-93.
105. Lee, G.D., et al., *Dietary deprivation extends lifespan in Caenorhabditis elegans*. *Aging Cell*, 2006. **5**(6): p. 515-24.
106. Haigis, M.C. and L.P. Guarente, *Mammalian sirtuins--emerging roles in physiology, aging, and calorie restriction*. *Genes Dev*, 2006. **20**(21): p. 2913-21.
107. Ristow, M., *Unraveling the truth about antioxidants: mitohormesis explains ROS-induced health benefits*. *Nat Med*, 2014. **20**(7): p. 709-11.
108. Vairetti, M., et al., *Apoptosis vs. necrosis: glutathione-mediated cell death during rewarming of rat hepatocytes*. *Biochim Biophys Acta*, 2005. **1740**(3): p. 367-74.
109. Onken, B. and M. Driscoll, *Metformin induces a dietary restriction-like state and the oxidative stress response to extend C. elegans Healthspan via AMPK, LKB1, and SKN-1*. *PLoS One*, 2010. **5**(1): p. e8758.
110. Tapia, P.C., *Sublethal mitochondrial stress with an attendant stoichiometric augmentation of reactive oxygen species may precipitate many of the beneficial alterations in cellular physiology produced by caloric restriction, intermittent fasting, exercise and dietary phytonutrients: "Mitohormesis" for health and vitality*. *Med Hypotheses*, 2006. **66**(4): p. 832-43.
111. Markaki, M. and N. Tavernarakis, *Modeling human diseases in Caenorhabditis elegans*. *Biotechnol J*, 2010. **5**(12): p. 1261-76.
112. McIntire, S.L., et al., *The GABAergic nervous system of Caenorhabditis elegans*. *Nature*, 1993. **364**(6435): p. 337-41.
113. Chen, Y., et al., *Subunit composition of a DEG/ENaC mechanosensory channel of Caenorhabditis elegans*. *Proc Natl Acad Sci U S A*, 2015. **112**(37): p. 11690-5.
114. Huang, M. and M. Chalfie, *Gene interactions affecting mechanosensory transduction in Caenorhabditis elegans*. *Nature*, 1994. **367**(6462): p. 467-70.
115. Goodman, M.B., et al., *MEC-2 regulates C. elegans DEG/ENaC channels needed for mechanosensation*. *Nature*, 2002. **415**(6875): p. 1039-42.
116. Zhang, W., et al., *Intersubunit interactions between mutant DEG/ENaCs induce synthetic neurotoxicity*. *Cell Death Differ*, 2008. **15**(11): p. 1794-803.
117. Chatzigeorgiou, M., et al., *Spatial asymmetry in the mechanosensory phenotypes of the C. elegans DEG/ENaC gene mec-10*. *J Neurophysiol*, 2010. **104**(6): p. 3334-44.
118. Liu, B., et al., *SIRT4 Prevents Hypoxia-Induced Apoptosis in H9c2 Cardiomyoblast Cells*. *Cell Physiol Biochem*, 2013. **32**(3): p. 655-62.
119. Sack, M.N. and T. Finkel, *Mitochondrial metabolism, sirtuins, and aging*. *Cold Spring Harb Perspect Biol*, 2012. **4**(12).

120. Donmez, G., et al., *SIRT1 protects against alpha-synuclein aggregation by activating molecular chaperones*. J Neurosci, 2012. **32**(1): p. 124-32.
121. Yang, Y., et al., *New role of silent information regulator 1 in cerebral ischemia*. Neurobiol Aging, 2013. **34**(12): p. 2879-88.
122. Jeong, J.K., et al., *Autophagy induced by the class III histone deacetylase Sirt1 prevents prion peptide neurotoxicity*. Neurobiol Aging, 2013. **34**(1): p. 146-56.
123. George, J. and N. Ahmad, *Mitochondrial Sirtuins in Cancer: Emerging Roles and Therapeutic Potential*. Cancer Res, 2016. **76**(9): p. 2500-6.
124. Swanson, R.A., *Astrocyte glutamate uptake during chemical hypoxia in vitro*. Neurosci Lett, 1992. **147**(2): p. 143-6.
125. Sato, E., et al., *Sodium azide induces necrotic cell death in rat squamous cell carcinoma SCC131*. Med Mol Morphol, 2008. **41**(4): p. 211-20.
126. Starich, T.A., et al., *Mutations affecting the chemosensory neurons of Caenorhabditis elegans*. Genetics, 1995. **139**(1): p. 171-88.
127. Hall, D.H., et al., *Neuropathology of degenerative cell death in Caenorhabditis elegans*. J Neurosci, 1997. **17**(3): p. 1033-45.
128. Syntichaki, P., et al., *Specific aspartyl and calpain proteases are required for neurodegeneration in C. elegans*. Nature, 2002. **419**(6910): p. 939-44.
129. Magni, G., et al., *Enzymology of NAD⁺ synthesis*. Adv Enzymol Relat Areas Mol Biol, 1999. **73**: p. 135-82, xi.
130. Revollo, J.R., et al., *Nampt/PBEF/Visfatin regulates insulin secretion in beta cells as a systemic NAD biosynthetic enzyme*. Cell Metab, 2007. **6**(5): p. 363-75.
131. Vrablik, T.L., et al., *Nicotinamidase modulation of NAD⁺ biosynthesis and nicotinamide levels separately affect reproductive development and cell survival in C. elegans*. Development, 2009. **136**(21): p. 3637-46.
132. van der Horst, A., et al., *The Caenorhabditis elegans nicotinamidase PNC-1 enhances survival*. Mech Ageing Dev, 2007. **128**(4): p. 346-9.
133. Gallo, C.M., D.L. Smith, Jr., and J.S. Smith, *Nicotinamide clearance by Pnc1 directly regulates Sir2-mediated silencing and longevity*. Mol Cell Biol, 2004. **24**(3): p. 1301-12.
134. Huang, L. and W. Hanna-Rose, *EGF signaling overcomes a uterine cell death associated with temporal mis-coordination of organogenesis within the C. elegans egg-laying apparatus*. Dev Biol, 2006. **300**(2): p. 599-611.
135. Crook, M., et al., *An NAD(+) biosynthetic pathway enzyme functions cell non-autonomously in C. elegans development*. Dev Dyn, 2014. **243**(8): p. 965-76.
136. Haigis, M.C., et al., *SIRT4 inhibits glutamate dehydrogenase and opposes the effects of calorie restriction in pancreatic beta cells*. Cell, 2006. **126**(5): p. 941-54.
137. Tissenbaum, H.A., *Serotonin's SOS signal*. Cell Metab, 2006. **4**(6): p. 415-7.